© 2023. Published by The Company of Biologists Ltd | Journal of Experimental Biology (2023) 226, jeb245355. doi:10.1242/jeb.245355

RESEARCH ARTICLE

The roles of brain lipids and polar metabolites in the hypoxia tolerance of deep-diving pinnipeds

Gerrit A. Martens[1,*], Cornelia Geßner[1], Lars P. Folkow[2], Marina Creydt[3], Markus Fischer[3] and Thorsten Burmester[1]

ABSTRACT

Lipids make up more than half of the human brain's dry weight, yet the composition and function of the brain lipidome is not well characterized. Lipids not only provide the structural basis of cell membranes, but also take part in a wide variety of biochemical processes. In neurodegenerative diseases, lipids can facilitate neuroprotection and serve as diagnostic biomarkers. The study of organisms adapted to extreme environments may prove particularly valuable in understanding mechanisms that protect against stressful conditions and prevent neurodegeneration. The brain of the hooded seal (*Cystophora cristata*) exhibits a remarkable tolerance to low tissue oxygen levels (hypoxia). While neurons of most terrestrial mammals suffer irreversible damage after only short periods of hypoxia, *in vitro* experiments show that neurons of the hooded seal display prolonged functional integrity even in severe hypoxia. How the brain lipidome contributes to the hypoxia tolerance of marine mammals has been poorly studied. We performed an untargeted lipidomics analysis, which revealed that lipid species are significantly modulated in marine mammals compared with non-diving mammals. Increased levels of sphingomyelin species may have important implications for efficient signal transduction in the seal brain. Substrate assays also revealed elevated normoxic tissue levels of glucose and lactate, which suggests an enhanced glycolytic capacity. Additionally, concentrations of the neurotransmitters glutamate and glutamine were decreased, which may indicate reduced excitatory synaptic signaling in marine mammals. Analysis of hypoxia-exposed brain tissue suggests that these represent constitutive mechanisms rather than an induced response towards hypoxic conditions.

KEY WORDS: Lipidome, Hypoxia, Oxidative stress, Marine mammals, Pinniped, Brain

INTRODUCTION

Lipids account for more than half of the dry weight of the human brain. However, their significance in cell metabolism has been underestimated in the past, as they have been dismissed as fixed building blocks of cell membranes and energy reserves (Lehninger, 1981; Fitzner et al., 2020). Recently, more and more studies show that lipids function as signalling molecules in the human brain, as neurotransmitters and growth factors (Piomelli et al., 2007). Lipidomics studies aim to describe the complete lipid profile (lipidome) in a cell, tissue or even whole organism. Advances in experimental techniques, such as mass spectrometry, allow the comprehensive analysis of lipid species. Nevertheless, the composition and function of the brain lipidome is not well characterized in any species (Fitzner et al., 2020). The main lipids detected in the human brain include glycerophospholipids, sphingolipids and cholesterol (O'Brien and Sampson, 1965). Reduced brain lipid content has been found in neurodegenerative diseases such as Alzheimer's disease, and lipids are therefore increasingly used as diagnostic biomarkers and drug targets (Buccellato et al., 2021; Castellanos et al., 2021). Lipidomics has further been suggested as a tool to study the evolution of marine mammals as well as to monitor their health status (Rey et al., 2022). For this purpose, two independent studies have linked the blubber and plasma lipid profiles of beluga whales (*Delphinapterus leucas*) with their physiology and health state, such as inflammatory processes (Bernier-Graveline et al., 2021; Tang et al., 2018). Furthermore, lipids such as neuroprotectin D1 have been shown to reduce inflammation and apoptosis in human neuronal glial cells (Zhao et al., 2011). Studying organisms adapted to extreme environments may shed light on mechanisms that protect them from specific stress conditions that might otherwise cause neurodegeneration and which could be of relevance in a broader context. Hooded seals (*Cystophora cristata*) and harp seals (*Pagophilus groenlandicus*) spend most of their time at sea, where they perform occasional long dives to exploit underwater food resources in shallow to deep waters. The hooded seal routinely dives to relatively deep waters ranging from 100 to 600 m for a duration of 5 to 15 min, but may dive deeper than 1 km and for durations over 1 h (Folkow and Blix, 1999; Andersen et al., 2013; Vacquie-Garcia et al., 2017). The harp seal usually dives to shallower depths of 50–100 m, lasting 5–15 min, but dives beyond 500 m depth have also been recorded (Folkow et al., 2004). Physiological adaptations, such as elevated oxygen stores (haemoglobin, myoglobin) and a dramatic redistribution of the blood supply involving profound peripheral vasoconstriction and bradycardia, have evolved to enable this diving lifestyle (Scholander, 1940; Ponganis, 2011; Blix, 2018; Ramirez et al., 2007). However, during repetitive diving bouts, arterial oxygen partial pressure may drop dramatically to levels that could cause neuronal damage in humans (Lutz, 2002), as has been demonstrated in some other seal species (Meir et al., 2009; Qvist et al., 1986). Neurons from the hooded seal have been shown to display intrinsic tolerance properties to low oxygen conditions (hypoxia) that cannot be explained by the global physiological adaptations mentioned above. Thus, isolated hooded seal brain slices maintained both membrane potential and functional integrity (synaptic transmission) during and after exposure to severe hypoxia that resulted in loss of functional integrity in non-diving species (Folkow et al., 2008;

[1]Institute of Animal Cell and Systems Biology, Biocenter Grindel, University of Hamburg, 20146 Hamburg, Germany. [2]Department of Arctic and Marine Biology, University of Tromsø – The Arctic University of Norway, Breivika, NO 9037 Tromsø, Norway. [3]Hamburg School of Food Science, Institute of Food Chemistry, University of Hamburg, 20146 Hamburg, Germany.

*Author for correspondence (gerrit.a.martens@gmail.com)

G.A.M., 0000-0002-5101-6796

Received 28 November 2022; Accepted 13 March 2023

Ramirez et al., 2011; Geiseler et al., 2016). As major components of membranes, specific neuronal lipids of diving mammals could contribute to the observed high hypoxia tolerance.

Changes in lipid structure, composition and abundance have contributed to the adaptation of marine mammals to an aquatic environment (see Strandberg et al., 2008; Liwanag et al., 2012). Divergent evolution of lipid metabolism in cetacean species is evident in positive selection, lineage-specific patterns of amino acid substitutions and functional domains in genes associated with lipid digestion, lipid storage and energy-producing pathways (Endo et al., 2018). In the visual cortex of hooded seals, two genes involved in lipid metabolism (*gdpd2*, *psap*) were among the most highly expressed genes when compared with the expression profile of a carnivoran relative, the ferret (*Mustela putorius furo*) (Fabrizius et al., 2016). A genome analysis of the Weddell seal (*Leptonychotes weddellii*) and the walrus (*Odobenus rosmarus*), revealed that genes related to lipid metabolism are enriched in regions of accelerated divergence in both these pinnipeds compared with 57 other placental mammals, which strongly suggests an important role of certain lipids in their adaptation to life in the marine environment (Noh et al., 2022). Remarkable lipid transport capabilities have been determined in the serum of the Weddell seal as evidenced by high levels of circulating cholesterol in a high-density lipoprotein (HDL)-like particle (Noh et al., 2022). Kasamatsu et al. (2009) demonstrated that serum cholesterol levels were elevated in bottlenose dolphins (*Tursiops truncatus*) and spotted seals (*Phoca largha*) compared with aquatic (West Indian manatees, *Trichechus manatus*) and terrestrial relatives (cows and dogs). Total cholesterol for marine mammals may be as high as 393 mg dl^{-1} in adult male northern elephant seals (*Mirounga angustirostris*), but decreases to 266 mg dl^{-1} after a 3 month fasting period during the breeding season (Tift et al., 2011), while normal total cholesterol level in man (*Homo sapiens*) is 200 mg dl^{-1} (Goodman, 1988). Interestingly, levels of antioxidative HDL were maintained during the breeding fast, which may prevent damage associated with oxidative stress (Tift et al., 2011). Similar serum cholesterol values have been reported for other cetacean (Venn-Watson et al., 2008; Nabi et al., 2019; Kasamatsu et al., 2012; Lauderdale et al., 2021; Mello et al., 2021) and pinniped species (Kohyama and Inoshima, 2017; Mazzaro et al., 2003). However, cholesterol levels vary according to season and age in cetacean species (Norman et al., 2013; Nollens et al., 2019, 2020; Tsai et al., 2016) and increase in response to physical stress, as shown in killer whales (*Orcinus orca*) (Steinman et al., 2020). Hence, tightly regulated lipid mobilization may be necessary for pinniped lifestyle, for example, during extended fasting periods during development, moulting, breeding and lactation (Nordøy et al., 1993; Fowler et al., 2018).

In pinniped species, the fatty acid composition of plasma, milk, blubber, liver and muscle has been studied (Dannenberger et al., 2020; Simond et al., 2022; Watson et al., 2021), but data on the lipid composition of the pinniped brain and its potential involvement in hypoxia tolerance is not available. Data for cetacean species is more extensive, in which the lipidomes of plasma (Tang et al., 2018; Monteiro et al., 2021b), heart (Monteiro et al., 2021a), liver (Simond et al., 2022) and blubber (Bories et al., 2021; Bernier-Graveline et al., 2021; Ruiz-Hernández et al., 2022; Simond et al., 2020) have already been analysed. Furthermore, Glandon et al. (2021) studied the lipid profile of neural tissue (brain, spinal cord, and spinal nerves) of stranded cetaceans in comparison to non-diving species (pigs, sheep). Lipid content, lipid class composition, and fatty acid signature were found to be similar across species, which may reflect a consistent functional role of lipids in the neural tissues of mammals (Glandon et al., 2021). However, specific fatty acids were not comprehensively analysed because of sample size constraints and limited availability of tissue.

Recently, it has been suggested that the lipid composition of membranes facilitates metabolic suppression in hypoxia-tolerant species by regulating activity of proteins important for ion flux (Farhat and Weber, 2021). Reducing energy consumption has obvious beneficial effects under conditions of low oxygen and energy supply and is a well-known strategy to which several specialized species resort. For instance, the activity of the plasma-membrane-localized sodium/potassium ATPase (Na^+/K^+-ATPase), an ATP-dependent ion pump, may be responsible for 20–70% of the oxygen expenditure of mammalian cells (Lee et al., 2020). Consequently, hypoxia-tolerant species such as crucian carp (*Carassius carassius*) and its close relative, the goldfish (*Carassius auratus*), the naked mole rat (*Heterocephalus glaber*) and the pond slider turtle (*Trachemys scripta*) have been shown to downregulate brain Na^+/K^+-ATPase in response to hypoxic conditions (Hylland et al., 1997; Farhat et al., 2021a,b), possibly by altering the abundance of certain fatty acids and cholesterol (Farhat et al., 2019, 2020; Farhat and Weber, 2021). Interestingly, genes involved in ion transport were found to be downregulated in fresh visual cortex slices of the hooded seal that had been exposed to hypoxia and reoxygenation *in vitro* (Hoff et al., 2017). Thus, in response to these stress conditions, the hooded seal brain may also decrease neuronal processes to reduce energy expenditure (see Ramirez et al., 2007). Additionally, membrane lipid composition may influence glycolytic activity and mitochondrial function, but the underlying mechanisms are not well understood (Farhat and Weber, 2021).

To improve our understanding of potential lipid-linked adaptations of hypoxia-tolerant species, we performed an untargeted lipidomics study comparing the brain lipidome of two marine mammals, the hooded seal and the harp seal, with those of two non-diving species, the ferret and the house mouse (*Mus musculus*). Furthermore, we compared the lipidome of hooded seal brain tissue that had been incubated under artificial normoxic and hypoxic conditions as well as being reoxygenated after a hypoxic period, which provokes oxidative stress. Additionally, we determined substrate levels for energy metabolism and neurotransmission in brain tissue samples.

MATERIALS AND METHODS

Animals and sampling

Hooded seals (*Cystophora cristata*) and harp seals (*Pagophilus groenlandicus*) were captured for other scientific purposes in March 2017 (n=3 hooded seal juveniles of both sexes), 2018 (n=1 weaned hooded seal pup, n=2 adult hooded seal females, n=3 adult harp seal females), 2019 (n=4 adult hooded seal females, n=3 adult harp seal females, n=6 hooded seal juveniles of both sexes) and 2021 (n=4 adult hooded seal females) in the pack ice of the Greenland Sea under permits from relevant Norwegian and Greenland authorities. The hooded seal pups caught in 2017 and 2019 were brought to UiT, The Arctic University of Norway, where they were maintained in a certified research animal facility in connection with other studies. At the termination of those experiments, the seals were euthanized (in 2019 and 2020, as juveniles, at age ∼2 years and ∼1 year, respectively) according to the following protocol: the seals were sedated by intramuscular injection of zolazepam/tiletamine (Zoletil Forte, Virbac S.A., France; 1.5–2.0 mg kg^{-1} body mass), then anaesthetized using an endotracheal tube to ventilate lungs with 2–3% isoflurane (Forene, Abbott, Germany) in air and, when fully anaesthetized, they were euthanized by exsanguination via the carotid arteries. The adult hooded and harp seals were euthanized

Journal of Experimental Biology (2023) 226, jeb245355. doi:10.1242/jeb.245355

immediately following capture with a hoop net, by sedation with intramuscular injection of zolazepam/tiletamine (1.5–2.0 mg per kg of body mass), followed by catheterization of the extradural intravertebral vein and i.v. injection of an overdose of pentobarbital (Euthasol vet., Le Vet, Netherlands; 30 mg kg^{-1} body mass). The animal study was reviewed and approved by the Norwegian Animal Welfare Act and with permits from the National Animal Research Authority of Norway and Norwegian Food Safety Authority (permits no. 7247, 19305 and 22751).

Samples of adult female ferrets (n=4) were received from the animal facilities of the University Medical Center Hamburg-Eppendorf (UKE) Germany. The ferrets were killed at the UKE in deep anaesthesia (Ketamin/Domitor) with an overdose of pentobarbital and brain tissues were sampled by the facility's veterinarians. Adult female mice (C57BL/6, n=9) were a gift from Prof. Dr Christian Lohr (University of Hamburg, Hamburg, Germany) and were anaesthetized with 1 ml isoflurane (Forene, Abbott, Germany) in a chamber and decapitated. All animals were handled according to the EU Directive 63 (Directive 2010/63/EU). For lipidomics of tissue exposed to hypoxia and reoxygenation, fresh visual cortex and hippocampus samples from hooded seal pups caught in 2019, as well as fresh visual cortex samples from hooded seal adults caught in 2021, were minced and placed in cooled (4°C) artificial cerebrospinal fluid (aCSF; 128 mmol l^{-1} NaCl, 3 mmol l^{-1} KCl, 1.5 mmol l^{-1} $CaCl_2$, 1 mmol l^{-1} $MgCl_2$, 24 mmol l^{-1} $NaHCO_3$, 0.5 mmol l^{-1} NaH_2PO_4, 20 mmol l^{-1} sucrose, 10 mmol l^{-1} D-glucose) saturated with 95% O2, 5% CO_2 (normoxia) and further processed *in vitro*, as described below. For lipidomics and metabolite assays of normoxic tissue, fresh tissue of the visual cortex of all animals was frozen in liquid nitrogen and transferred to −80°C to be stored for subsequent analysis. An overview of samples used in each study is provided in Table 1.

Hypoxia and reoxygenation treatment of brain samples

Samples in oxygenated (95% O_2, 5% CO_2) aCSF were adjusted to 34±0.5°C for at least 20 min. Hypoxia was introduced and maintained for 60 min after switching the gas supply to 95% N_2 and 5% CO_2, to mimic the conditions in the brain during a dive. To simulate conditions when the seal surfaces after a dive, samples were exposed to hypoxia followed by return to normoxia (95% O_2, 5% CO_2) for 20 min. After treatment, hypoxia and reoxygenation samples were immediately frozen in liquid nitrogen. Samples that were kept under normoxia in aCSF for 80 min were used as controls. All samples were transferred to and stored at −80°C until later use.

Table 1. Sample overview for each study

Study	Animals	Number
LC-MS lipidomics comparison of marine versus terrestrial mammals	Harp seal – adults	6
	Hooded seal – juveniles	4
	Hooded seal – adults	6
	Mouse – adults	9
	Ferret – adults	4
LC-MS lipidomics comparison of hypoxia-treated hooded seal brain samples	Hooded seal – juveniles	6
	Hooded seal – adults	4
Substrate comparison of marine versus terrestrial mammals	Harp seal – adults	3
	Hooded seal – adults	4
	Mouse – adults	4
Substrate comparison of hypoxia-treated hooded seal brain samples	Hooded seal – juveniles	5
	Hooded seal – adults	4

Animals and number of samples for each study are provided.

Chemicals for mass spectrometry

Acetonitrile, isopropanol, methanol (all LC–MS grade), chloroform (HPLC grade), ammonium formate (≥95% puriss) and sodium hydroxide (≥99%) were purchased from Carl Roth GmbH (Karlsruhe, Germany). Formic acid (99% p.a.) and acetic acid (99% p.a.) were provided by Acros Organics (Geel, Belgium). Hexakis(1H,1H,2H-perfluoroethoxy)phosphazene was supplied by Santa Cruz Biotechnology (Dallas, TX, USA). Water was obtained by a Merck Millipore water purification system with a resistance of 18 MΩ (Darmstadt, Germany).

Extraction procedure for mass spectrometry

Extraction of metabolites and further analysis was performed at Hamburg School of Food Science, University of Hamburg. The extraction protocol was performed slightly modified according to the method of Bligh and Dyer (Bligh and Dyer, 1959; Creydt et al., 2018). Approximately 20 mg of sample was weighed into a 2.0 ml reaction tube (Eppendorf, Hamburg, Germany). Two steel balls (3.6 mm), 100 µl chloroform and 200 µl methanol were added to the sample. The mixture was homogenized in a ball mill (1 min, 3.1 m s^{-1} Bead Ruptor 24, Omni International IM, GA, USA). Next, 200 µl water and 100 µl chloroform were added and again processed in the ball mill (1 min, 3.1 m s^{-1}). The homogenized sample was then centrifuged (20 min, 16,000 ***g***, 5°C, Sigma 3-16PK, Sigma, Osterode, Germany). A quality control sample (QC) was prepared by transferring 30 µl of each sample into a new vial. The organic chloroform phase was directly used for measurement.

Mass spectrometric data acquisition

High-performance liquid chromatography coupled with electrospray ionization-quadrupole-time of flight-mass spectrometry (LC–ESI–qTOF–MS/MS) was used for metabolite identification as described previously (Creydt et al., 2018). In brief, the LC experiments were carried out using a RP C-18 column (150×2.1 mm, 1.7 µm, Phenomenex, Aschaffenburg, Germany) together with a Dionex Ultimate 3000 UPLC system (Dionex, Idstein, Germany). The mobile phase consisted of water (solvent A) and mixture of acetonitrile and isopropanol (1:3, v/v) (solvent B). Both eluents contained 10 mmol l^{-1} ammonium formate for measurements in positive ionization mode and 0.02% acetic acid for measurements in negative ionization mode. The column oven was set at 50°C and the flow rate was 300 µl min^{-1}. The gradient elution was as follows: 55% B (0–2 min); 55% to 75% B (2–4 min); 75% to 100% B (4–18 min); 100% B (18–23 min), 55% B (23–24 min); 55% B (24–27 min). For measurements in positive ionization mode, 2 µl of the sample extracts were injected, whereas for analyses in negative ionization mode, 8 µl were used. The samples were analysed in randomized order, with one blank sample and one QC sample being measured after each of the five animal samples. The autosampler in which the samples were stored during the measurement was set to 4°C.

The LC system was connected to an ESI–qTOF–MS (maXis 3G, Bruker Daltonics, Bremen, Germany). The data were recorded at 1 Hz over a mass range of m/z 80–1100. Further parameters were: end plate offset, −500 V; capillary, −4500 V (positive mode), +4500 V (negative mode); nebulizer pressure, 4.0 bar; dry gas, 9.0 l min^{-1} at 200°C dry temperature. At the beginning of the measurements, the mass spectrometer was calibrated either using sodium formate clusters or sodium acetate clusters, depending on which additive was used in the solvent. At the end of each sample run, a further calibration was carried out using the cluster solutions. In the MS/MS measurements for the identification of the substances,

hexakis(1H,1H,2H-perfluoroethoxy)phosphazene was used as lock mass during the entire measurement period. The recording of MS/MS spectra was carried out at 20, 40 and 60 eV.

Metabolomics data analysis

Acquired experimental mass spectra were recalibrated with Bruker Data Analysis Software 4.2 (Bruker Daltonics, Bremen, Germany) using the sodium formate clusters for *m/z* ratios acquired in positive ionization mode and the sodium acetate clusters for *m/z* ratios acquired in negative ionization mode. Then, data were exported to netCDF file format. Data preprocessing was performed with R package xcms 3.6.2 (https://xcmsonline.scripps.edu/; Smith et al., 2006) in R version 3.6.3 (https://www.r-project.org/). Parameters for processing were optimized based on existing tools and scripts (Libiseller et al., 2015; Manier et al., 2019). After reading in recalibrated netCDF files, features were detected with findChromPeaks function and CentWaveParam [peakwidth=c(10,40), ppm=20, snthresh=10, mzdiff=0.015, prefilter=c(0,0), noise=0]. Retention time was corrected with adjustRtime function and ObiwarpParam (binSize=1.0). Feature correspondence was achieved with groupChromPeaks function and PeakDensityParam (sampleGroups=xdata$sample_group, bw=1) as well as missing value imputation with fillChromPeaks function with FillChromPeaksParam (fixedRt=ChromPeakwidth/2). ChromPeakwidth was calculated as average peak width of detected chromatographic peaks. Adducts and isotopes of features were annotated using the R package CAMERA 1.40.0 (Kuhl et al., 2012). Features in the QC samples with a relative standard deviation over 30%, blank intensity contribution over 10% and QC sample count below 60% were removed before further statistical analysis.

Statistical analysis

Peak intensity tables with two sample groups (marine/terrestrial) were uploaded to MetaboAnalyst 4.0 software (Xia et al., 2009; Chong et al., 2019) and intensities were subjected to sum normalization and log-transformation. For univariate analysis of features, fold change calculation and *t*-test were performed. Features were considered significant with a false discovery rate (FDR) below P=0.05. Furthermore, unsupervised multivariate analysis (PCA) and supervised multivariate analysis (PLS-DA) were calculated. Cross validation (CV) was executed with the 10-fold CV method to confirm PLS-DA models. Variable importance plot (VIP) scores of features in PLS-DA over 1 were used to further assess significant features.

Compound annotation

Significant features were annotated with MS/MS spectra using the *in silico* fragmentation tool metfRag 2.4.2 (https://ipb-halle.github.io/MetFrag/). Chromatographic peaks were identified with the R package xcms 3.6.2 (Smith et al., 2006) as described above and isotopes and adducts of chromatographic peaks annotated with CAMERA 1.40.0 (Kuhl et al., 2012). If multiple MS/MS spectra per chromatographic peak were available, consensus spectra of MS/MS spectra were built with combineSpectra function (method=consensusSpectrum, mzd=0.001, minProp=0.8, intensityFun=median, mzFun=median). Consensus spectra and exact mass from CAMERA annotation were searched with metfRag against the LipidMaps database (Wolf et al., 2010). Search settings were: DatabaseSearchRelativeMassDeviation: 10.0, FragmentPeakMatchAbsoluteMassDeviation: 0.005, Fragment PeakMatchRelativeMassDeviation: 10.0. Annotation reliability of non-polar candidate substances was additionally improved with LipidFrag software (Witting et al., 2017). A MetFrag as well as LipidFrag score of 1.0 represents a likely lipid identification. Example spectra of identified lipids are provided in Fig. S1. After identification, lipid set enrichment analysis regarding lipid class, chain length and unsaturation was performed with the lipidr package (https://www.lipidr.org). Briefly, samples were subjected to sum normalization and log-transformation in MetaboAnalyst 4.0 software (https://www.metaboanalyst.ca), as described previously. Differential analysis was then conducted with de_analysis function and enrichment determined with lsea function. A heatmap was generated with MetaboAnalyst 5.0 (Pang et al., 2021) using the normalized data and feature autoscaling. Euclidean distance measure and Ward clustering method were used for hierarchical clustering of samples.

Substrate assays

About 20 mg of frozen brain sample was rinsed with phosphate buffered saline, transferred into a cryo vial with 1.4 mm ceramic beads and homogenized in 50 mmol l^{-1} tris(hydroxymethyl)aminomethane with 0.6 N HCl at an 8:1 ratio using a Fisherbrand™ Bead Mill 4 Homogenizer for 20 s at maximum speed (Thermo Fisher Scientific, Waltham, MA, USA). Samples were mixed with one eighth volume of 1 mol l^{-1} Tris-HCl, centrifuged (1500 ***g***, 5 min) and supernatant used in Glucose-Glo™, Lactate-Glo™ and Glutamine/Glutamate-Glo™ Assays after manufacturer's instructions (Promega, Mannheim, Germany). Protein concentration of samples was determined by Bradford Assay using Roti®Quant solution (Carl Roth, Karlsruhe, Germany) and a bovine serum albumin standard curve (Carl Roth). Luminescence of substrate assays and absorption of Bradford Assay were measured with a DTX 880 Multimode Detector (Beckmann Coulter, Krefeld, Germany). Substrate concentration was normalized to total protein concentration and statistically analysed with the compare_means function of the ggpubr package (https://CRAN.R-project.org/package=ggpubr) in R version 4.1.2 (https://www.r-project.org/). Briefly, two sample *t*-tests were performed on the normally distributed data using one reference group (mouse or normoxia samples, respectively) and additionally adjusting *P*-values with the Benjamini–Hochberg method (FDR).

RESULTS

Lipidomics of marine and terrestrial brain samples

Mass spectrometry data of hooded seals (*Cystophora cristata*), harp seals (*Pagophilus groenlandicus*), ferrets (*Mustela putorius furo*) and mice (*Mus musculus*) tissues from the visual cortex were collected. After splitting into marine and terrestrial mammals, PLS-DA demonstrated distinct lipidomic patterns for these groups (Fig. 1). The Q^2 value of the cross-validation of the measurements in the positive mode and in the negative mode were 0.98 and 0.97, respectively. Both values accordingly indicate large differences in the samples.

Of 4072 features detected in positive ionization mode and 5720 features detected in negative ionization mode, 201 and 313 features were significantly different between marine and terrestrial mammals, respectively. After removal of low quality and isotope features, a total of 230 features (pos: 85; neg: 145) were selected for annotation by MS/MS spectra. Of 44 (pos: 29; neg: 15) annotated features (Table S1), 3 were duplicate annotations of separate features, resulting in 41 unique annotated metabolites.

The majority of annotated metabolites represented lipid classes from major components of biological membranes, such as phosphatidylcholines (PCs) with 23 features,

Journal of Experimental Biology (2023) 226, jeb245355. doi:10.1242/jeb.245355

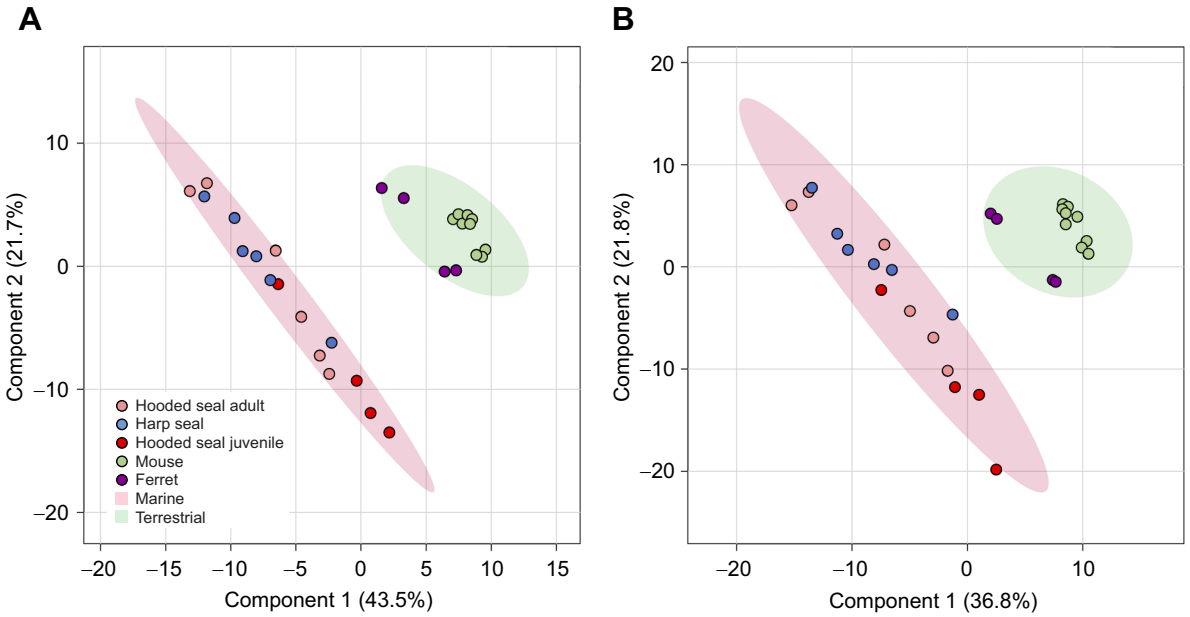

Fig. 1. Supervised multivariate analysis of the mass spectrometry analyses of marine mammals compared with terrestrial mammals. Supervised multivariate analysis (PLS-DA) of high-performance liquid chromatography coupled with electrospray ionization-quadrupole-time of flight-mass spectrometry (LC–ESI–qTOF–MS/MS) analyses performed in (A) positive ionization and (B) negative ionization mode. Marine mammals included hooded seal adults (n=6), hooded seal juveniles (n=4) and harp seals (n=6) and terrestrial mammals included ferrets (n=4) and mice (n=9).

phosphatidylethanolamines (PE) with 8 lipids and phosphatidylserines (PSs) with 3 features and phosphatidylinositols (PIs) with 2 annotated features (Table 2). Other classes included lipids involved in myelin sheath formation, such as sphingomyelin (SM) with 7 features and one signal probably representing a cerebroside (HexCer). While these single lipids demonstrated significant differences between marine and terrestrial mammals, fold change of whole lipid classes was not significant between groups (Fig. S2). Nevertheless, detected lipid classes appeared to be generally increased in the marine mammals (Fig. 2). SMs for example were on average 6 times higher [binary logarithm of fold change ($\log_2$FC)=2.6] and the two PIs demonstrated an average 8-fold increase ($\log_2$FC=3.0). The only detected HexCer was 9-fold ($\log_2$FC=3.2) elevated, whereas the other lipid classes did not show a comparable increase (PC: $\log_2$FC=2.0; PE: $\log_2$FC=1.7; PS: $\log_2$FC=1.0). Notably, 19 out of 23 PC species were significantly increased in marine mammals. Additionally, we detected a substantial amount of phospholipid plasmalogen species (PC-O and PE-O), in which fatty acids are linked to the phospholipid backbone by an alkyl or alkenyl ether instead of an ester bond. Of the 14 identified plasmalogen lipids, 12 demonstrated higher concentrations in marine mammals and an average 5-fold increase ($\log_2$FC=2.4). However, in enrichment analyses with only the subset of plasmalogen species, no significant accumulation in the marine mammals could be determined (Fig. S3).

Both lipid unsaturation and chain length influence membrane fluidity and rigidity. Adaptation of marine mammals to cold environments may have selected for lipids of shorter chain length and a higher amount of double bonds to maintain membrane fluidity. However, unsaturation of lipids (Fig. S4) and lipid chain length (Fig. S5) were not significantly different between marine and terrestrial mammals. We noted that a total chain unsaturation of 4 double bonds and a total chain length of 38 carbon atoms appeared to be decreased in seals compared with ferret and

Table 2. Overview of annotated lipid classes

Lipid class	No.	Function
Glycerophospholipids		
Phosphatidylcholine (PC)	23	Major component of biological membranes, creating a planar lipid bilayer (van Meer et al., 2008)
Phosphatidylethanolamine (PE)	8	Major component of biological membranes, mainly found in the inner (cytoplasmic) leaflet of the lipid bilayer; regulation of membrane curvature and thereby role in membrane budding, fission and fusion (van Meer et al., 2008)
Phosphatidylinositol (PI)	2	Minor component on the cytosolic side of eukaryotic cell membranes, important roles in lipid signalling, cell signalling and membrane trafficking (Di Paolo and Camilli, 2006)
Phosphatidylserine (PS)	3	Localized exclusively in the cytoplasmic leaflet of biological membranes. Its exposure on the outer surface of a membrane acts as a signal for phagocytosis and consequently apoptosis (Schlegel and Williamson, 2001)
Sphingolipids		
Sphingomyelin (SM)	7	Part of animal cell membranes, especially in the insulating membranous myelin sheath that surrounds some nerve cell axons; involved in signal transduction (Schneider et al., 2019); hydrolyses into ceramide (Kolesnick, 1994)
Neutral glycosphingolipids/ cerebrosides (HexCer)	1	Important component of animal nerve cell membranes, regulating nerve myelin sheath formation or remyelination (Jurevics et al., 2001)

Number of identified significant detections and functional descriptions are provided for each lipid class.

Journal of Experimental Biology (2023) 226, jeb245355. doi:10.1242/jeb.245355

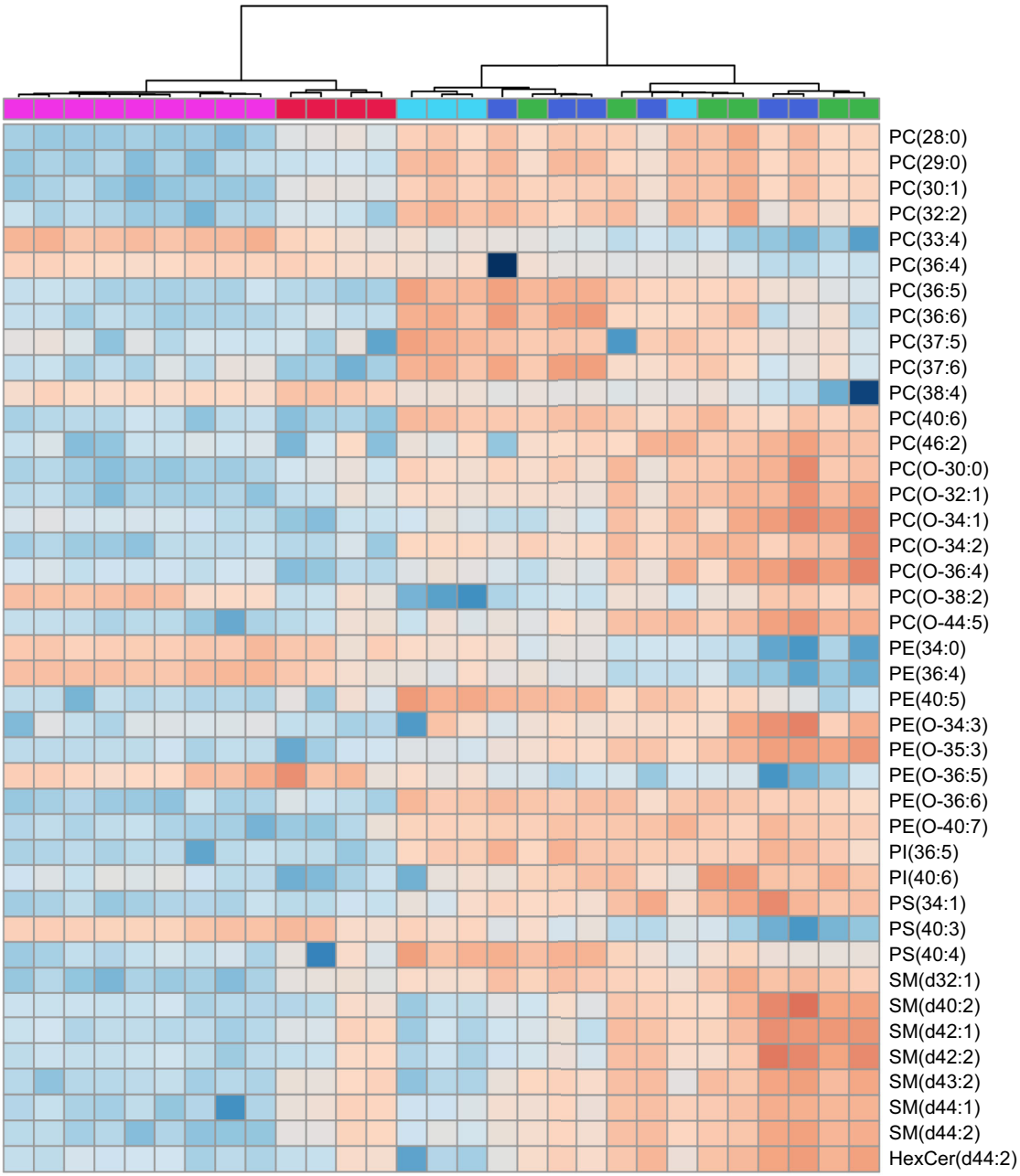

Fig. 2. Heat map of identified significant lipid species with hierarchical clustering of samples. Samples are categorized by species and age class. Lipid classes include: PC, phosphatidylcholine; PE, phosphatidylethanolamine; PI, phospatidylinositol; PS, phosphatidylserine; SM, sphingomyelin; HexCer, cerebroside.

mice, whereas other unsaturation indices and chain lengths tended to be increased.

Metabolite assays of marine and terrestrial mammals

Analysis of molecules from energy metabolism (glucose and lactate) and synaptic transmission (glutamate and glutamine) revealed substantial differences between hooded and harp seals on the one hand, and mice on the other (Fig. 3). Normalized glucose levels were significantly higher in the hooded seal cerebellum (FDR, $P<0.01$) and visual cortex (FDR, $P<0.05$), whereas they were only marginally higher in the harp seal cerebellum and visual cortex, and hooded seal hippocampus, when compared with mice. Furthermore, concentration of lactate was significantly higher in the hooded seal (FDR, $P<0.0001$) and harp seal hippocampus (FDR, $P<0.05$), as well as in the hooded seal visual cortex (FDR, $P<0.01$), compared with mice. On the other hand, the levels of the neurotransmitters glutamine and glutamate were generally lower in seals compared with mice. Glutamate levels were significantly lower in the hooded seal cortex (FDR, $P<0.001$) and glutamine levels were significantly lower in the hooded seal cerebellum (FDR, $P<0.001$), harp seal hippocampus (FDR, $P<0.05$) and hooded seal visual cortex (FDR, $P<0.001$). In this regard, it is important to remember that the metabolic/oxygenation state of the sampled animals and tissues sampled was not fully known, although the effects of handling the animals and samples can be predicted to some degree, as discussed in more detail in the Discussion.

Journal of Experimental Biology (2023) 226, jeb245355. doi:10.1242/jeb.245355

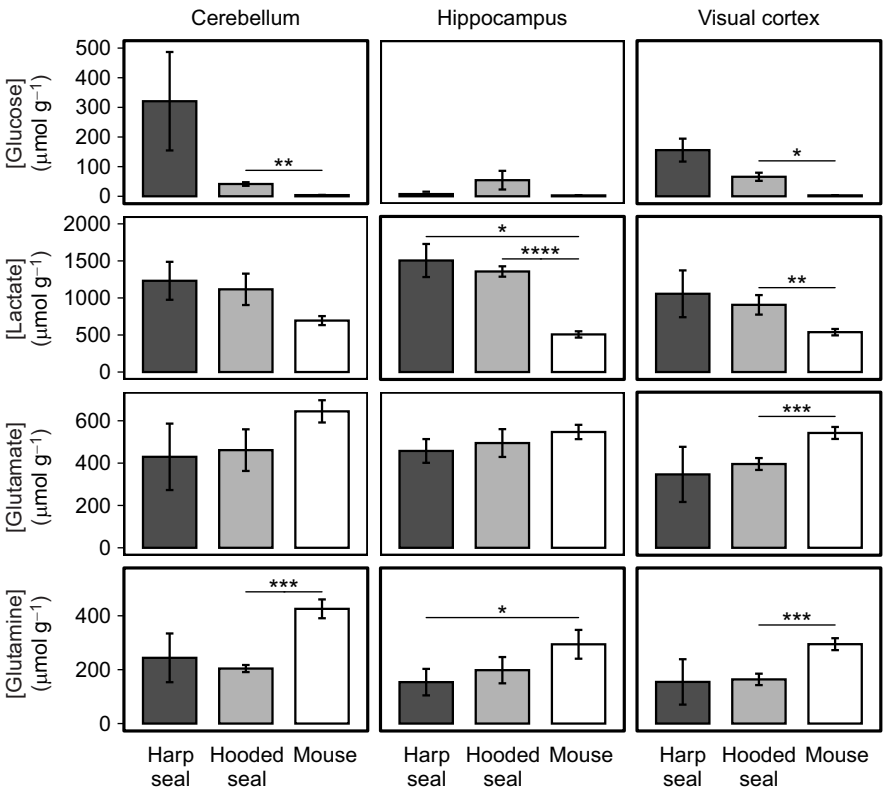

Fig. 3. Substrate assays of marine mammals compared with terrestrial mammals. Substrate concentrations (mean±s.d.) of glucose, lactate, glutamate and glutamine were normalized to total protein concentration in the harp seal (*n*=3), hooded seal (*n*=4) and mouse (*n*=4) visual cortex, hippocampus and cerebellum, respectively. Statistical analysis was performed with two-sample *t*-tests including Benjamini–Hochberg correction (FDR). **P*<0.05, ***P*<0.01, ****P*<0.001, *****P*<0.0001.

Lipidomics and metabolite assays of hypoxia- and reoxygenation-treated hooded seal brain samples

Fresh juvenile hooded seal visual cortices and hippocampi and adult hooded seal visual cortices were maintained *in vitro* at different oxygen regimes to emulate conditions of hypoxia and reoxygenation that hooded seals are frequently exposed to. Untargeted lipidomics analysis did not reveal significantly changed lipid levels for the different treatments. Cross validation of the PLS-DA analyses demonstrated poor predictive Q^2 values of −0.68 and 0.46, in the positive and negative mode, respectively, for the treated juvenile hooded seal brain tissue (Fig. 4A,B) and −0.04 and 0.12, in the positive and negative mode, respectively, for the treated adult hooded seal brain tissue (Fig. 4C,D). Group separation by lipid concentration therefore is inconclusive. Nevertheless, some significant differences in lactate, glutamate and glutamine concentrations were determined with substrate assays, while glucose levels were maintained across conditions and did not show significant differences between treatments (Fig. 5). Lactate levels were significantly lower in the visual cortex of juvenile hooded seals after reoxygenation compared with levels in normoxia (FDR, P<0.01), whereas they were insignificantly lower after hypoxic treatment only. The same trend was found in the visual cortex of adult hooded seals, but differences were not significant. The concentration of glutamate was significantly lower in the hippocampus of juvenile hooded seals after reoxygenation (FDR, P<0.01), but not after hypoxia compared with normoxia. Similarly, glutamate appears to be insignificantly lower in the visual cortex of juvenile and adult hooded seals after reoxygenation and to a lesser extent after hypoxia compared with normoxia. Glutamine levels decreased after hypoxia, but almost recovered to normoxic levels after reoxygenation. Significant differences compared with normoxia were therefore only found after hypoxic treatment of the visual cortex of juvenile (FDR, P<0.01) and adult hooded seals (FDR, P<0.01).

Samples that were subjected to *in vitro* incubation in aCSF under known oxygenation conditions, had a known metabolic history that is defined by the oxygenation conditions to which they were experimentally subjected (normoxia, hypoxia or hypoxia followed by reoxygenation). We here must assume that the 20 min pre-incubation of tissue in fully oxygenated aCSF was sufficient to ‘reset’ cells to a normoxic metabolic state, should their metabolic/oxygenation state have been disturbed because of the prior handling (animal capture procedure and metabolic effects of drugs).

DISCUSSION

Lipids are ubiquitous in the brain, yet the composition and function of the brain lipidome is not well characterized (Fitzner et al., 2020). They not only provide the structural basis of cell membranes, but also take part in a wide variety of vital tasks in the brain including signal transduction (Piomelli et al., 2007). In neurodegenerative diseases, lipids may facilitate neuroprotection and serve as diagnostic biomarkers (Zhao et al., 2011; Castellanos et al., 2021). While neurons of most terrestrial (non-diving) mammals suffer irreversible damage after only short periods of low tissue oxygen levels (hypoxia), *in vitro* experiments revealed that neurons of the hooded seal show prolonged functional integrity during hypoxic conditions (Folkow et al., 2008; Geiseler et al., 2016). How the brain lipidome may contribute to the hypoxia tolerance of diving mammals has not been comprehensively studied. In this study, we performed an untargeted lipidomics analysis, which revealed that some lipid species are significantly modulated in marine mammals in comparison to terrestrial mammals. Furthermore, some metabolites involved in energy metabolism and neurotransmission appear to be regulated differently in marine than in terrestrial mammals.

The metabolic/oxygenation state of sampled tissues

The conditions to which the animals were exposed prior to sampling affect the metabolic/oxygenation state of the sampled tissues, and

Journal of Experimental Biology (2023) 226, jeb245355. doi:10.1242/jeb.245355

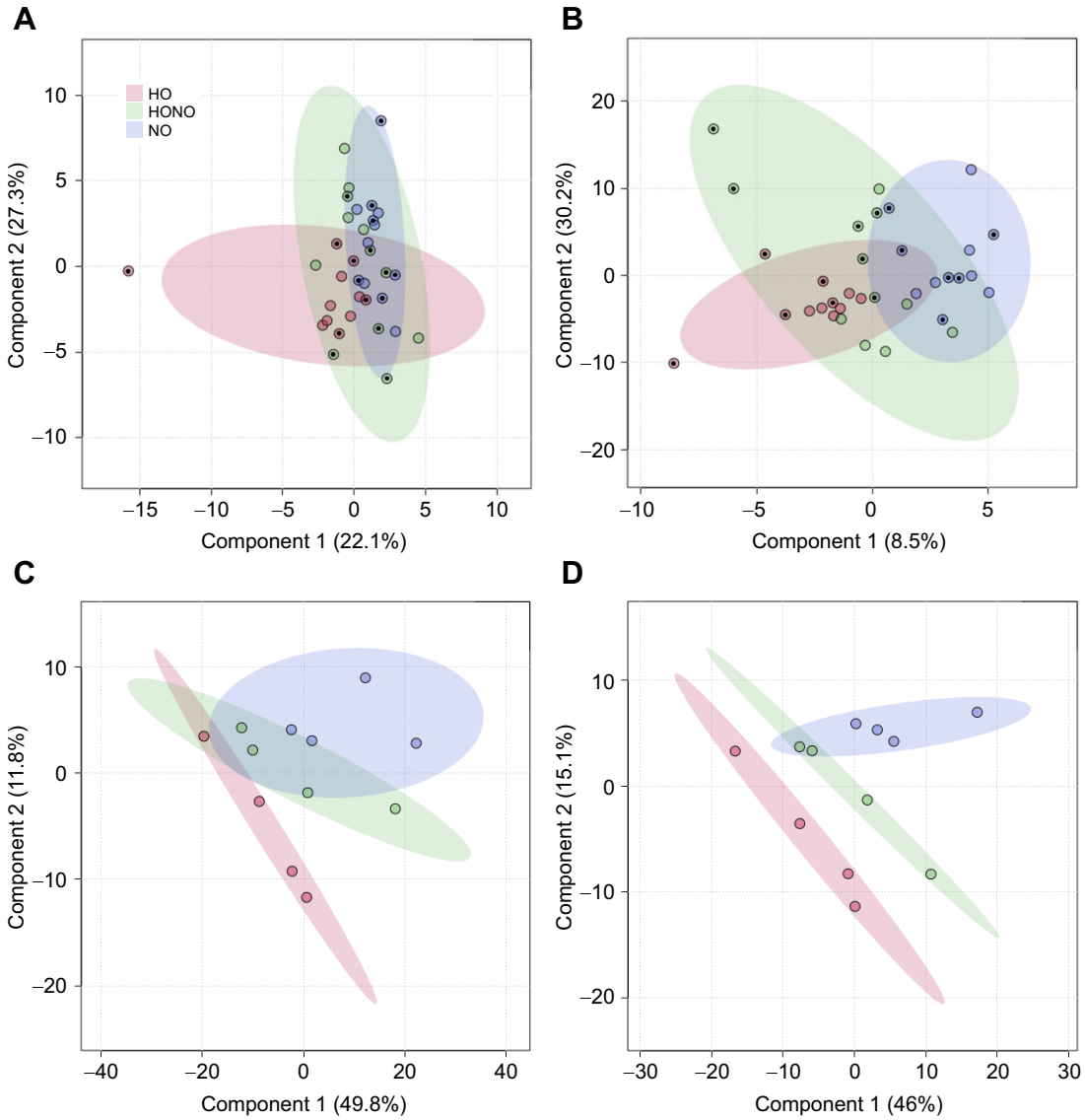

Fig. 4. Supervised multivariate analysis of the mass spectrometry analyses of the hooded seal brain exposed to different oxygen regimes. Juvenile hooded seal (*n*=6) hippocampi and visual cortices (visual cortex samples marked with black dots) were exposed to normoxia (NO), hypoxia (HO) and reoxygenation (HONO) and analysed in (A) positive ionization and (B) negative ionization mode. Similarly, adult hooded seal (*n*=4) visual cortices were exposed to normoxia (NO), hypoxia (HO) and reoxygenation (HONO) and analysed in (C) positive ionization and (D) negative ionization mode.

this must be taken into account when interpreting data. This presumably concerns tissue metabolite and neurotransmitter levels, in particular. Unfortunately, we were unable to determine tissue oxygenation levels, but have made the following theoretical analysis of the possible effects of the various treatments.

All animals were captured and restrained before sedation, anaesthesia and euthanasia. Capture and restraint involves a certain amount of physical effort and thus represents a stressful situation for the animals, which could affect the metabolic state of the sampled brain tissue. However, even in the case of live capture of adult seals, the capture procedure only involved moderate temporal and intense exertion for the animal, as animals typically resigned shortly (1–2 min) after being entrapped and were then immediately sedated with drugs having induction times of <1 min (Wheatley et al., 2006). During the ∼10 min interval until sedated animals were catheterized and euthanized, or intubated and manually ventilated (as was the case for some of the seals), spontaneous ventilation was somewhat depressed, presumably causing very moderate hypoxia (particularly from a seal perspective). However, manual ventilation (isoflurane in air) of those seals concerned rapidly restored normal oxygenation levels (>95% O_2 saturation), as confirmed with a pulse oximeter with sensor attached to tongue. In other species (rats and humans), isoflurane, pentobarbital, ketamine (a close relative to tiletamine, which we used) and diazepam (a close relative to zolazepam, which we used) are all known to reduce brain glucose uptake (Prando et al., 2019; Kelly et al., 1986), and to depress cerebral brain metabolic rate as a whole (de Wit et al., 1991). Since all brain tissues that were collected immediately after euthanasia were under the influence of one or more of the drugs mentioned above, we may assume that their metabolic/oxygenation state was comparable.

In contrast, those samples that were subjected to *in vitro* incubation in aCSF under known oxygenation conditions, had a known metabolic history that is defined by the oxygenation conditions to which they were experimentally subjected (normoxia, hypoxia or hypoxia followed by reoxygenation). Here, we assume that the

Journal of Experimental Biology (2023) 226, jeb245355. doi:10.1242/jeb.245355

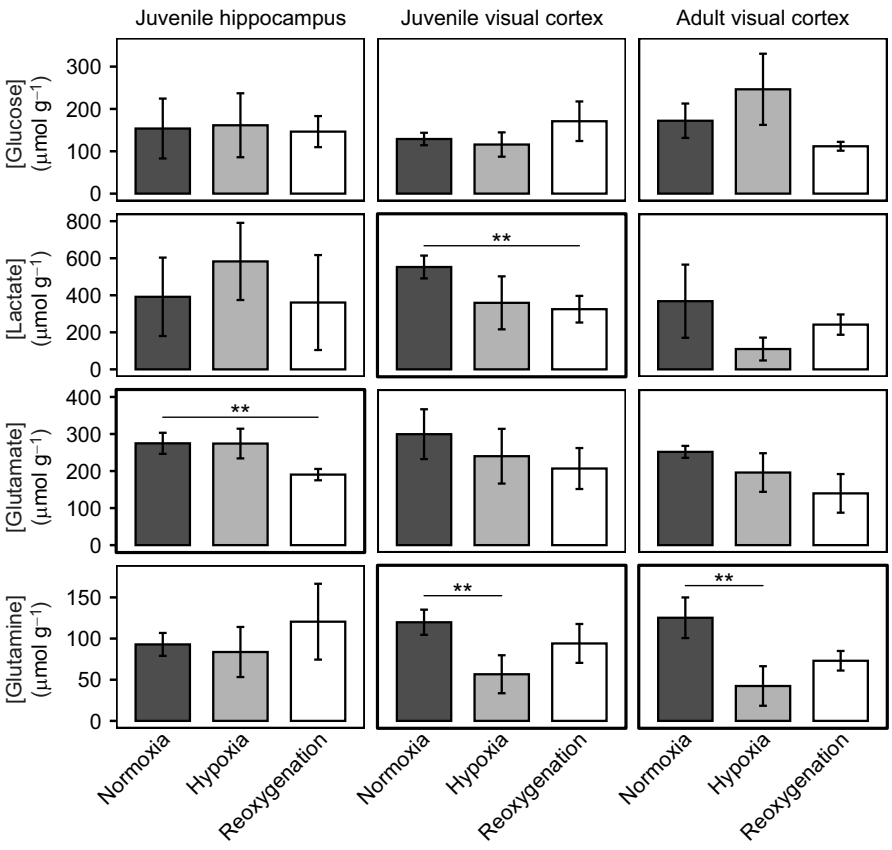

Fig. 5. Substrate assays of the hooded seal brain exposed to different oxygen regimes. Substrate concentrations (mean±s.d.) of glucose, lactate, glutamate and glutamine were normalized to total protein concentration in visual cortex and hippocampus of juvenile hooded seals (n=5) and visual cortex of adult hooded seals (n=4) exposed to normoxia, hypoxia and reoxygenation, respectively. Statistical analysis was performed with two-sample t-tests including Benjamini–Hochberg correction (FDR). *P<0.05, ** P<0.01, *** P<0.001, **** P<0.0001.

20 min pre-incubation of tissue in fully oxygenated aCSF was sufficient to 'reset' cells to a normoxic metabolic state, should their metabolic/oxygenation state have been disturbed by the prior handling (animal capture procedure and metabolic effects of drugs).

Lipids and neurotransmission

Sphingolipids, especially sphingomyelin, form the myelin sheath surrounding axons and are thereby directly involved in signal transduction in the brain (Schneider et al., 2019). Myelin insulates nerve fibres, decreasing the capacitance and increasing the electrical resistance across the axonal membrane, thereby enabling rapid saltatory conduction of action potentials (Hartline, 2008). We observed that sphingolipids such as cerebroside and sphingomyelin are mainly elevated in the seal brain compared with levels in mice and ferrets, but a general significant increase of one lipid class could not be determined. A stronger sheathing of the axon would further reduce the capacitance of the axonal membrane and produce a faster conduction speed, as well as allowing a smaller number of ions to enter the fibre, thereby reducing the metabolic cost of pumping ions across the membrane (Hartline, 2008). Reducing energy consumption and thereby oxygen demand may be beneficial under low oxygen conditions, as routinely experienced during diving of seals. Apart from myelin formation and signal transduction, sphingolipids can modulate various biological processes such as growth, cell migration, adhesion, apoptosis, senescence and inflammation (Hannun and Obeid, 2018). Additionally, sphingolipids can be transformed into each other. For instance, sphingomyelin can be hydrolysed to form ceramide, which has apoptotic functions as described below (Kolesnick, 1994). Ceramides may also induce negative membrane curvature, which might promote budding and vesiculation, thereby contributing to synaptic signalling (van Blitterswijk et al., 2003). Because of the variety of functions and dynamic character of sphingolipids, a general role in the hooded seal brain is not easily ascribed. However, elevated levels of sphingolipids may contribute to efficient signal transduction and reduction of energy consumption.

Glutamate is the most abundant excitatory neurotransmitter in the vertebrate nervous system (Meldrum, 2000). Synaptically released glutamate is usually rapidly taken up from the extracellular space, to terminate its action (Schousboe, 1981). However, energy deficiency during hypoxia leads to glutamate accumulation in the synaptic cleft, which is a major contributor to excitotoxic cell death due to excessive calcium influx and neuronal depolarization (Belov Kirdajova et al., 2020; Choi and Rothman, 1990). Blocking of glutamate receptors resulted in a delayed depolarization of neurons in hippocampal slices of mice during anoxic challenge, preventing the initiation of cell death cascades (Heit et al., 2021). In this study, we found that the neurotransmitters glutamate and its predecessor glutamine were generally decreased in the seal brain compared with the mouse brain. Furthermore, we observed that glutamine, and to a lesser extent glutamate levels decreased in response to hypoxia in the hooded seal visual cortex. Since glutamatergic signalling and the recycling of the neurotransmitters are highly energy-intensive processes (Attwell and Laughlin, 2001), a reduction in glutamatergic signalling may be beneficial to (i) reduce energy expenditure that is limited during hypoxia and (ii) prevent neurotoxic events caused by failed glutamate reuptake from the synaptic cleft when ATP is limited under hypoxic conditions. Accordingly, a comparative transcriptomics analysis revealed that genes involved in glutamatergic transmission, e.g. glutamate receptors, were expressed at significantly lower levels, whereas genes involved in glutamate reuptake were more highly expressed in hooded seal neurons than in neurons of mice (Geßner et al., 2022). Ramirez et al. (2007) suggested that the brain of

diving mammals may survive hypoxic events through depression (partial 'shut-down') of neuronal activity during diving. Later, Buck and Pamenter (2018) proposed the 'synaptic arrest' hypothesis, stating that hypoxia-tolerant species have a lower basal expression of synaptic proteins and are able to decrease their function during periods of hypoxia. Regardless of mechanism, this would lead to decreased energy expenditure during low oxygen conditions. In accordance, a reduction in glutamate and glutamine has been observed in the hypoxia-tolerant naked mole rat (*Heterocephalus glaber*) brain in response to hypoxia but only glutamine decreases in the hypoxic mouse brain (Cheng et al., 2022). Interestingly, hypoxia preconditioning of mice also led to a decrease in glutamate, whereas inhibitory neurotransmitters, including γ-aminobutyric acid (GABA), dopamine, adenosine and taurine were increased in the hippocampus (Liao et al., 2018). In conclusion, reduced glutamatergic signalling in the seal brain may facilitate neuronal survival during hypoxic conditions by reducing energy expenditure and neurotoxic effects.

Ceramides and mitochondrial membrane function

Ceramides are waxy lipid molecules composed of sphingosine and a fatty acid, and they accumulate as a result of different stressors. For instance, ischemia increases ceramide levels in mouse brain tissue (Yu et al., 2000) and hypoxia induces ceramide synthesis in neuronal precursor cells (Jin et al., 2008) and neuroblastoma cells (Kang et al., 2010). Furthermore, altered ceramide metabolism is associated with various neurodegenerative diseases such as Alzheimer's disease, Parkinson's disease and Huntington's disease (Czubowicz et al., 2019). Ceramides are especially involved in modulating membrane processes and function in mitochondria (van Blitterswijk et al., 2003). They can influence the permeability of mitochondrial membranes (Siskind et al., 2002; Dadsena et al., 2019), leading to the release of aqueous contents of mitochondria such as cytochrome *c*, which in turn may induce apoptosis (Ghafourifar et al., 1999; Di Paola et al., 2000; Tsujimoto and Shimizu, 2000; Shimizu et al., 1999). However, the subcellular localization as well as chain length essentially influence the biological effect of ceramide species (Fugio et al., 2020). Short chain C2-ceramide (Parra et al., 2008) as well as long-chain C18-ceramide (Sentelle et al., 2012) may induce apoptosis, whereas CerS2-derived very long chain C20–C24-ceramides may lead to protective mitophagy (Law et al., 2018). Mitophagy is the selective autophagy of dysfunctional mitochondria to reduce cellular stress (Pickles et al., 2018). Consequently, ceramides reduce mitochondrial respiratory chain processes (Di Paola et al., 2000; Gudz et al., 1997).

Here, we found that sphingomyelins, which may be transformed into ceramides by acid sphingomyelinase (ASM), are increased in harp and hooded seals. Inhibition of ASM during glutamate-induced excitotoxicity in oligodendrocytes reduced ceramide levels and enhanced cell survival (Novgorodov et al., 2018). Additionally, knockout of ASM reduced mitochondrial defects, augmented the autophagic flux and improved the brain function recovery after traumatic brain injury (Novgorodov et al., 2019). Whether ASM is particularly active in marine mammals, thereby creating increased ceramide concentration from high levels of sphingomyelin is unknown. Nevertheless, in this study, the detected sphingomyelins had an average fatty acid chain length of 20–21 carbon atoms. Hydrolysation would therefore result in very long chain ceramides that could lead to mitophagy and thus reduced mitochondrial aerobic respiration (Kolesnick, 1994; Law et al., 2018). Depending on the reference organism and the depth of analyses, the capacity for aerobic respiration in the hooded seal visual cortex has been shown to be decreased or increased compared with terrestrial mammals (Fabrizius et al., 2016; Geßner et al., 2022). Thus, while the transcriptome of the visual cortex (whole tissue) indicated a reduced capacity for aerobic metabolism compared with ferrets (*Mustela putorius furo*) (Fabrizius et al., 2016), a more detailed neuron-specific analysis (of excised cortical neurons) demonstrated an elevated capacity in hooded seal neurons when compared with those of mice (Geßner et al., 2022). Similarly, an increased aerobic capacity was found in the cetacean brain when compared with cattle (*Bos taurus*) brains (Krüger et al., 2020). A metabolic analysis of the hibernating Syrian hamster (*Mesocricetus auratus*) brain revealed a reversible increase of ceramides in torpor animals, which might reflect increased mitophagy during hibernation and thus processes to prevent oxidative damage (Gonzalez-Riano et al., 2019). In contrast, we could not determine a lipidomic stress response by hypoxia treatment of seal brain tissue, which might point to a constitutive rather than an induced adaptation.

Energy metabolism of glucose and lactate

At normoxic conditions, glycolytic processes might be enhanced in the seal brain, as reflected by high glucose as well as lactate levels compared with levels in the mouse brain, at least as measured in our metabolite assays. Since these values are likely to reflect near-resting metabolite levels and since the possible drug effects on tissue metabolic state presumably were comparable between species (see 'The metabolic/oxygenation state of sampled tissues'), the noted species difference may reflect a pre-adaptation of the seal brain to upcoming stress conditions, not least since elevated brain glucose levels are considered to be neuroprotective (Swanson and Choi, 1993; Choi and Gruetter, 2003). Recently, it has been shown that the brain not only relies on glucose as the sole energy source, but can also efficiently metabolize other substrates, such as lactate (Bélanger et al., 2011). Typically, lactate is formed by glycolysis in astrocytes and subsequently transported into neurons, which convert lactate into pyruvate and utilize it in aerobic respiration to meet their high energy demands, as proposed by the 'astrocyte–neuron lactate shuttle' hypothesis (Pellerin and Magistretti, 1994). Interestingly, the hooded seal brain exhibits an unusual distribution of cytochrome *c*, neuroglobin and lactate dehydrogenase b in astrocytes rather than in neurons (Mitz et al., 2009; Hoff et al., 2016). Mitz et al. (2009) therefore proposed the 'reverse lactate shuttle' hypothesis, in which, at normoxic conditions, lactate is shuttled to astrocytes from basically anaerobic neurons, to be converted into pyruvate and subsequently used for aerobic respiration. This would protect oxidative stress-susceptible neurons by shifting oxidative metabolism to astrocytes.

During hypoxic conditions, lactate may be transported out of the brain to limit its (glial) oxidative metabolism and its detrimental effects. An increase of the lactate level in the cerebral venous effluent has already been observed at the end of long dives of harbour seals (*P. vitulina*) (Kerem and Elsner, 1973). In agreement, lactate concentration may have dropped in the adult and juvenile visual cortex, whereas glucose levels stayed approximately the same in our hypoxia- and reoxygenation-treated samples, possibly aided by the elevated brain glycogen stores of hooded seals (Czech-Damal et al., 2014). Czech-Damal et al. (2014) observed extended spontaneous neuronal activity in brain slices of hooded seal compared with mice, when exposed to hypoxia and ischemia, as well as in the presence of lactate. Interestingly, the monocarboxylate transporter *mct4* has been shown to be upregulated in response to hypoxia and reoxygenation in the hooded seal brain and may perform lactate efflux (Hoff et al., 2017). Generally high levels of *mct4* have been also found in hooded seal neurons in comparison to mouse

neurons (Geßner et al., 2022). However, neither of these transcriptomics studies (Hoff et al., 2017; Geßner et al., 2022) suggested any distinct regulation in cerebral glucose metabolism. Nevertheless, removal of lactate may be beneficial during low oxygen conditions and may contribute to the hypoxia tolerance of the hooded seal brain. Subsequently, tissues not as sensitive to pH changes and high buffering capacities may be able to deal with high lactate concentrations (Boutilier et al., 1993; Castellini and Somero, 1981).

Lipid saturation and membrane fluidity

Alterations in membrane lipid composition might be attributed to maintenance of adequate membrane fluidity (homeoviscous adaptations, see Hazel, 1990). To maintain membrane fluidity in cold environments, cell membranes of marine mammals, which display substantial peripheral heterothermia (e.g. Irving and Hart, 1957), might contain lipids of shorter chain lengths and with more double bonds. Williams et al. (2001) compared the erythrocyte membrane lipid composition from two deep-diving phocid seals (*M. angustirostris*, *P. vitulina*), with that of a relatively shallow-diving otariid seal (*Callorhinus ursinus*) and with non-diving mammals (*Canis familiaris*, *Equus caballus*, *Bos taurus*). Lipid unsaturation indices and proportions of long-chain polyunsaturated fatty acids (PUFAs) were substantially higher in the phocid seals, presumably linked to the necessity to maintain a fluid membrane in cold environments (Williams et al., 2001).

We observed no significant differences in cerebral lipid saturation (Fig. S4) or chain length (Fig. S5) between seals and non-diving mammals but noted that phospholipids with a total chain length of 38 carbon atoms tended to be decreased in marine mammals compared with terrestrial mammals. Since phospholipids contain two fatty acid chains, the average fatty acid chain length translates to 19 carbon atoms. The majority of fatty acids detected in the blubber (Wheatley et al., 2008) and muscle of Weddell seals were of similar chain lengths of 18 carbon atoms (Trumble et al., 2010), but in those studies, no comparison to terrestrial mammals was drawn. We also noted a non-significant decrease in moderately unsaturated lipids with four double bonds in marine mammals. For comparison, more than half of the detected fatty acids in skeletal muscle tissue of Weddell seals were monounsaturated fatty acids (MUFAs), which might be important for preventing ROS damage (Trumble et al., 2010). A comprehensive analysis of phospholipids in various rat organs suggests that brain phospholipids are least enriched with PUFAs compared with the heart, kidney and liver (Choi et al., 2018). Choi et al. (2018) argued that a decrease in membrane PUFAs might be a mechanism to protect from ischemic brain damage because of lower susceptibility to lipid peroxidation. Nevertheless, PUFAs are essential fatty acids, required for structural growth and brain development (Innis, 2005). Brain phospholipids are selectively enriched in specific PUFAs, especially arachidonic acid and docosahexaenoic acid (Bazinet and Layé, 2014), but their concentration may change with dietary intake (Chen et al., 2020) – a likely scenario for marine mammals with their lipid-rich diets. Consequently, Monteiro et al. (2021a) reported higher n-3 and lower n-6 fatty acid contents of small cetaceans [common dolphin (*Delphinus delphis*), harbour porpoise (*Phocoena phocoena*) and striped dolphin (*Stenella coeruleoalba*)] hearts compared with levels in hearts of their terrestrial relatives, reflecting the high availability of n-3 fatty acids in marine food chains.

Additionally, we detected a substantial amount of phospholipid plasmalogen species. The exact function of plasmalogen species remains obscure, but they are thought to act as antioxidants and facilitate membrane fusion (Dean and Lodhi, 2018). Furthermore, they reduce fluidity and improve rigidity of cell membranes by favouring close alignment of lipids (Dean and Lodhi, 2018; Braverman and Moser, 2012). In neurons of the human brain, phosphatidylethanolamine (PE) plasmalogen species constitute over 50% of total PEs (Han et al., 2001). Here, over 60% of detected PEs represented plasmalogen species. The antioxidative functions of plasmalogens might be beneficial and although they were at mostly increased concentrations in marine mammals, we could not determine a general accumulation of this lipid class.

Conclusions

Lipids are involved in a wide variety of biochemical pathways. In this study, we found that the brain lipidomes of diving mammals, the hooded seal and harp seal, differ from two terrestrial (non-diving) relatives, the mouse and ferret. Although single lipids are significantly regulated, whole lipid classes did not show a significant regulation. However, sphingomyelin species were generally increased in the seals compared with the terrestrial mammals, which may be important for efficient neuronal signal transduction. Excitatory synaptic signalling may be reduced in the seal brain, as illustrated by reduced levels of glutamate and glutamine. This could represent an adaptation to prevent neurotoxic events during hypoxia. Additionally, increased neural glucose and lactate levels may be suggestive of an elevated glycolytic capacity of the seal brain. Membrane fluidity and integrity are likely to play a substantial role in the adaptation of seals to the aquatic environment. However, we found no direct evidence of altered membrane lipid chain length or unsaturation between seals and terrestrial mammals. Hypoxia and reoxygenation treatment did not induce significant changes in the brain lipidome of hooded seals, but some metabolites (e.g. glutamine) were reduced in response to hypoxia. Therefore, not only a constitutive reduction in neurotransmitter levels and synaptic signalling, but also a further decrease in response to hypoxic conditions may contribute to the hypoxia tolerance of the hooded seal brain. The present study is the first to investigate the brain lipidome in specialized diving species and provides valuable insights into the hypoxia adaptations of the pinniped brain. Future studies could further explore how hypoxia and reoxygenation affect the brain lipidome as well as the polar substrates of diving compared with non-diving mammals.

Acknowledgements

Thanks are due to the crew of R/V *Helmer Hanssen* for their support in collecting hooded and harp seal samples.

Competing interests

The authors declare no competing or financial interests.

Author contributions

Conceptualization: T.B.; Methodology: G.A.M., C.G., L.P.F., M.C., M.F.; Software: G.A.M., M.C.; Validation: G.A.M., M.C.; Formal analysis: G.A.M., M.C.; Resources: L.P.F., M.F., T.B.; Data curation: G.A.M., M.C.; Writing - original draft: G.A.M.; Writing - review & editing: G.A.M., C.G., L.P.F., M.C., M.F.; Visualization: G.A.M.; Supervision: C.G.; Project administration: C.G.; Funding acquisition: T.B.

Funding

This work was supported by the Deutsche Forschungsgemeinschaft (Bu956/22).

Ethics approval

The animal study was reviewed and approved by the Norwegian Animal Welfare Act and with permits from the National Animal Research Authority of Norway and Norwegian Food Safety Authority (permits no. 7247, 19305 and 22751).

Data availability

Mass spectrometry data is available at the NIH Common Fund's National Metabolomics Data Repository (NMDR) website, the Metabolomics Workbench

(Sud et al., 2016) under Project ID PR001514. The data can be accessed directly via: http://dx.doi.org/10.21228/M80H6B.

References

Andersen, J. M., Skern-Mauritzen, M., Boehme, L., Wiersma, Y. F., Rosing-Asvid, A., Hammill, M. O. and Stenson, G. B. (2013). Investigating annual diving behaviour by hooded seals (*Cystophora cristata*) within the Northwest Atlantic Ocean. *PLoS ONE* **8**, e80438. doi:10.1371/journal.pone.0080438

Attwell, D. and Laughlin, S. B. (2001). An energy budget for signaling in the grey matter of the brain. *J. Cereb. Blood Flow Metab.* **21**, 1133-1145. doi:10.1097/00004647-200110000-00001

Bazinet, R. P. and Layé, S. (2014). Polyunsaturated fatty acids and their metabolites in brain function and disease. *Nat. Rev. Neurosci.* **15**, 771-785. doi:10.1038/nrn3820

Bélanger, M., Allaman, I. and Magistretti, P. J. (2011). Brain energy metabolism: focus on astrocyte-neuron metabolic cooperation. *Cell Metab.* **14**, 724-738. doi:10.1016/j.cmet.2011.08.016

Belov Kirdajova, D., Kriska, J., Tureckova, J. and Anderova, M. (2020). Ischemia-triggered glutamate excitotoxicity from the perspective of glial cells. *Front. Cell. Neurosci.* **14**, 51. doi:10.3389/fncel.2020.00051

Bernier-Graveline, A., Lesage, V., Cabrol, J., Lair, S., Michaud, R., Rosabal, M. and Verreault, J. (2021). Lipid metabolites as indicators of body condition in highly contaminant-exposed belugas from the endangered St. Lawrence Estuary population (Canada). *Environ. Res.* **192**, 110272. doi:10.1016/j.envres.2020.110272

Bligh, E. G. and Dyer, W. J. (1959). A rapid method of total lipid extraction and purification. *Can. J. Biochem. Physiol.* **37**, 911-917. doi:10.1139/o59-099

Blix, A. S. (2018). Adaptations to deep and prolonged diving in phocid seals. *J. Exp. Biol.* **221**, jeb182972. doi:10.1242/jeb.182972

Bories, P., Rikardsen, A. H., Leonards, P., Fisk, A. T., Tartu, S., Vogel, E. F., Bytingsvik, J. and Blévin, P. (2021). A deep dive into fat: Investigating blubber lipidomic fingerprint of killer whales and humpback whales in northern Norway. *Ecol. Evol.* **11**, 6716-6729. doi:10.1002/ece3.7523

Boutilier, R. G., Nikinmaa, M. and Tufts, B. L. (1993). Relationship between blood buffering properties, erythrocyte pH and water content, in gray seals (*Halichoerus grypus*). *Acta Physiol. Scand.* **147**, 241-247. doi:10.1111/j.1748-1716.1993.tb09495.x

Braverman, N. E. and Moser, A. B. (2012). Functions of plasmalogen lipids in health and disease. *Biochim. Biophys. Acta* **1822**, 1442-1452. doi:10.1016/j.bbadis.2012.05.008

Buccellato, F. R., D'anca, M., Fenoglio, C., Scarpini, E. and Galimberti, D. (2021). Role of oxidative damage in Alzheimer's disease and neurodegeneration: from pathogenic mechanisms to biomarker discovery. *Antioxidants (Basel, Switzerland)* **10**, 1353. doi:10.3390/antiox10091353

Buck, L. T. and Pamenter, M. E. (2018). The hypoxia-tolerant vertebrate brain: arresting synaptic activity. *Comp. Biochem. Physiol. B Biochem. Mol. Biol.* **224**, 61-70. doi:10.1016/j.cbpb.2017.11.015

Castellanos, D. B., Martín-Jiménez, C. A., Rojas-Rodríguez, F., Barreto, G. E. and González, J. (2021). Brain lipidomics as a rising field in neurodegenerative contexts: Perspectives with Machine Learning approaches. *Front. Neuroendocrinol.* **61**, 100899. doi:10.1016/j.yfrne.2021.100899

Castellini, M. A. and Somero, G. N. (1981). Buffering capacity of vertebrate muscle: Correlations with potentials for anaerobic function. *J. Comp. Physiol. B* **143**, 191-198. doi:10.1007/BF00797698

Chen, C. T., Haven, S., Lecaj, L., Borgstrom, M., Torabi, M., Sangiovanni, J. P. and Hibbeln, J. R. (2020). Brain PUFA concentrations are differentially affected by interactions of diet, sex, brain regions, and phospholipid pools in mice. *J. Nutr.* **150**, 3123-3132. doi:10.1093/jn/nxaa307

Cheng, H., Qin, Y. A., Dhillon, R., Dowell, J., Denu, J. M. and Pamenter, M. E. (2022). Metabolomic analysis of carbohydrate and amino acid changes induced by hypoxia in naked mole-rat brain and liver. *Metabolites* **12**, 56. doi:10.3390/metabo12010056

Choi, I.-Y. and Gruetter, R. (2003). In vivo 13C NMR assessment of brain glycogen concentration and turnover in the awake rat. *Neurochem. Int.* **43**, 317-322. doi:10.1016/S0197-0186(03)00018-4

Choi, D. W. and Rothman, S. M. (1990). The role of glutamate neurotoxicity in hypoxic-ischemic neuronal death. *Annu. Rev. Neurosci.* **13**, 171-182. doi:10.1146/annurev.ne.13.030190.001131

Choi, J., Yin, T., Shinozaki, K., Lampe, J. W., Stevens, J. F., Becker, L. B. and Kim, J. (2018). Comprehensive analysis of phospholipids in the brain, heart, kidney, and liver: brain phospholipids are least enriched with polyunsaturated fatty acids. *Mol. Cell. Biochem.* **442**, 187-201. doi:10.1007/s11010-017-3203-x

Chong, J., Wishart, D. S. and Xia, J. (2019). Using metaboanalyst 4.0 for comprehensive and integrative metabolomics data analysis. *Curr. Protoc. Bioinformatics* **68**, e86. doi:10.1002/cpbi.86

Creydt, M., Hudzik, D., Rurik, M., Kohlbacher, O. and Fischer, M. (2018). Food authentication: small-molecule profiling as a tool for the geographic discrimination of German white asparagus. *J. Agric. Food Chem.* **66**, 13328-13339. doi:10.1021/acs.jafc.8b05791

Czech-Damal, N. U., Geiseler, S. J., Hoff, M. L. M., Schliep, R., Ramirez, J.-M., Folkow, L. P. and Burmester, T. (2014). The role of glycogen, glucose and lactate in neuronal activity during hypoxia in the hooded seal (*Cystophora cristata*) brain. *Neuroscience* **275**, 374-383. doi:10.1016/j.neuroscience.2014.06.024

Czubowicz, K., Jęśko, H., Wencel, P., Lukiw, W. J. and Strosznajder, R. P. (2019). The role of ceramide and sphingosine-1-phosphate in Alzheimer's disease and other neurodegenerative disorders. *Mol. Neurobiol.* **56**, 5436-5455. doi:10.1007/s12035-018-1448-3

Dadsena, S., Bockelmann, S., Mina, J. G. M., Hassan, D. G., Korneev, S., Razzera, G., Jahn, H., Niekamp, P., Müller, D., Schneider, M. et al. (2019). Ceramides bind VDAC2 to trigger mitochondrial apoptosis. *Nat. Commun.* **10**, 1832. doi:10.1038/s41467-019-09654-4

Dannenberger, D., Möller, R., Westphal, L., Moritz, T., Dähne, M. and Grunow, B. (2020). Fatty acid composition in blubber, liver, and muscle of marine mammals in the southern Baltic sea. *Animals* **10**, 1509. doi:10.3390/ani10091509

De Wit, H., Metz, J., Wagner, N. and Cooper, M. (1991). Effects of diazepam on cerebral metabolism and mood in normal volunteers. *Neuropsychopharmacology* **5**, 33-41.

Dean, J. M. and Lodhi, I. J. (2018). Structural and functional roles of ether lipids. *Protein Cell* **9**, 196-206. doi:10.1007/s13238-017-0423-5

Di Paola, M., Cocco, T. and Lorusso, M. (2000). Ceramide interaction with the respiratory chain of heart mitochondria. *Biochemistry* **39**, 6660-6668. doi:10.1021/bi9924415

Di Paolo, G. and De Camilli, P. (2006). Phosphoinositides in cell regulation and membrane dynamics. *Nature* **443**, 651-657. doi:10.1038/nature05185

Endo, Y., Kamei, K. I. and Inoue-Murayama, M. (2018). Genetic signatures of lipid metabolism evolution in Cetacea since the divergence from terrestrial ancestor. *J. Evol. Biol.* **31**, 1655-1665. doi:10.1111/jeb.13361

Fabrizius, A., Hoff, M. L. M., Engler, G., Folkow, L. P. and Burmester, T. (2016). When the brain goes diving: transcriptome analysis reveals a reduced aerobic energy metabolism and increased stress proteins in the seal brain. *BMC Genomics* **17**, 583. doi:10.1186/s12864-016-2892-y

Farhat, E., Cheng, H., Romestaing, C., Pamenter, M. and Weber, J.-M. (2021a). Goldfish response to chronic hypoxia: mitochondrial respiration, fuel preference and energy metabolism. *Metabolites* **11**, 187. doi:10.3390/metabo11030187

Farhat, E., Devereaux, M. E. M., Cheng, H., Weber, J.-M. and Pamenter, M. E. (2021b). Na+/K+-ATPase activity is regionally regulated by acute hypoxia in naked mole-rat brain. *Neurosci. Lett.* **764**, 136244. doi:10.1016/j.neulet.2021.136244

Farhat, E., Devereaux, M. E. M., Pamenter, M. E. and Weber, J.-M. (2020). Naked mole-rats suppress energy metabolism and modulate membrane cholesterol in chronic hypoxia. *Am. J. Physiol. Regul. Integr. Comp. Physiol.* **319**, R148-R155. doi:10.1152/ajpregu.00057.2020

Farhat, E., Turenne, E. D., Choi, K. and Weber, J.-M. (2019). Hypoxia-induced remodelling of goldfish membranes. *Comp. Biochem. Physiol. B Biochem. Mol. Biol* **237**, 110326. doi:10.1016/j.cbpb.2019.110326

Farhat, E. and Weber, J.-M. (2021). Hypometabolic responses to chronic hypoxia: a potential role for membrane lipids. *Metabolites* **11**, 503. doi:10.3390/metabo11080503

Fitzner, D., Bader, J. M., Penkert, H., Bergner, C. G., Su, M., Weil, M.-T., Surma, M. A., Mann, M., Klose, C. and Simons, M. (2020). Cell-type- and brain-region-resolved mouse brain lipidome. *Cell Reports* **32**, 108132. doi:10.1016/j.celrep.2020.108132

Folkow, L. P. and Blix, A. S. (1999). Diving behaviour of hooded seals (*Cystophora cristata*) in the greenland and norwegian seas. *Polar Biol.* **22**, 61-74. doi:10.1007/s003000050391

Folkow, L. P., Nordy, E. S. and Blix, A. S. (2004). Distribution and diving behaviour of harp seals (*Pagophilus groenlandicus*) from the Greenland Sea stock. *Polar Biol.* **27**, 281-298. doi:10.1007/s00300-004-0591-7

Folkow, L. P., Ramirez, J.-M., Ludvigsen, S., Ramirez, N. and Blix, A. S. (2008). Remarkable neuronal hypoxia tolerance in the deep-diving adult hooded seal (*Cystophora cristata*). *Neurosci. Lett.* **446**, 147-150. doi:10.1016/j.neulet.2008.09.040

Fowler, M., Champagne, C. and Crocker, D. (2018). Adiposity and fat metabolism during combined fasting and lactation in elephant seals. *J. Exp. Biol.* **221** Suppl. 1, jeb161554. doi:10.1242/jeb.161554

Fugio, L. B., Coeli-Lacchini, F. B. and Leopoldino, A. M. (2020). Sphingolipids and mitochondrial dynamic. *Cells* **9**, 581. doi:10.3390/cells9030581

Geiseler, S. J., Larson, J. and Folkow, L. P. (2016). Synaptic transmission despite severe hypoxia in hippocampal slices of the deep-diving hooded seal. *Neuroscience* **334**, 39-46. doi:10.1016/j.neuroscience.2016.07.034

Geßner, C., Krüger, A., Folkow, L. P., Fehrle, W., Mikkelsen, B. and Burmester, T. (2022). Transcriptomes suggest that pinniped and cetacean brains have a high capacity for aerobic metabolism while reducing energy-intensive processes such as synaptic transmission. *Front. Mol. Neurosci.* **15**, 877349. doi:10.3389/fnmol.2022.877349

Ghafourifar, P., Klein, S. D., Schucht, O., Schenk, U., Pruschy, M., Rocha, S. and Richter, C. (1999). Ceramide induces cytochrome c release from isolated mitochondria. Importance of mitochondrial redox state. *J. Biol. Chem.* **274**, 6080-6084. doi:10.1074/jbc.274.10.6080

Glandon, H. L., Loh, A. N., Mclellan, W. A., Pabst, D. A., Westgate, A. J. and Koopman, H. N. (2021). Lipid signature of neural tissues of marine and terrestrial mammals: consistency across species and habitats. *J. Comp. Physiol. B* **191**, 815-829. doi:10.1007/s00360-021-01373-x

Gonzalez-Riano, C., León-Espinosa, G., Regalado-Reyes, M., García, A., Defelipe, J. and Barbas, C. (2019). Metabolomic study of hibernating Syrian hamster brains: in search of neuroprotective agents. *J. Proteome Res.* **18**, 1175-1190. doi:10.1021/acs.jproteome.8b00816

Goodman, D. S. (1988). Report of the national cholesterol education program expert panel on detection, evaluation, and treatment of high blood cholesterol in adults. *Arch. Intern. Med.* **148**, 36. doi:10.1001/archinte.1988.00380010040006

Gudz, T. I., Tserng, K. Y. and Hoppel, C. L. (1997). Direct inhibition of mitochondrial respiratory chain complex III by cell-permeable ceramide. *J. Biol. Chem.* **272**, 24154-24158. doi:10.1074/jbc.272.39.24154

Han, X., Holtzman, D. M. and Mckeel, D. W. (2001). Plasmalogen deficiency in early Alzheimer's disease subjects and in animal models: molecular characterization using electrospray ionization mass spectrometry. *J. Neurochem.* **77**, 1168-1180. doi:10.1046/j.1471-4159.2001.00332.x

Hannun, Y. A. and Obeid, L. M. (2018). Sphingolipids and their metabolism in physiology and disease. *Nat. Rev. Mol. Cell Biol.* **19**, 175-191. doi:10.1038/nrm.2017.107

Hartline, D. K. (2008). What is myelin? *Neuron Glia Biol.* **4**, 153-163. doi:10.1017/S1740925X09990263

Hazel, J. (1990). The role of alterations in membrane lipid composition in enabling physiological adaptation of organisms to their physical environment. *Prog. Lipid Res.* **29**, 167-227. doi:10.1016/0163-7827(90)90002-3

Heit, B. S., Dykas, P., Chu, A., Sane, A. and Larson, J. (2021). Synaptic and network contributions to anoxic depolarization in mouse hippocampal slices. *Neuroscience* **461**, 102-117. doi:10.1016/j.neuroscience.2021.02.021

Hoff, M. L. M., Fabrizius, A., Folkow, L. P. and Burmester, T. (2016). An atypical distribution of lactate dehydrogenase isoenzymes in the hooded seal (*Cystophora cristata*) brain may reflect a biochemical adaptation to diving. *J. Comp. Physiol. B* **186**, 373-386. doi:10.1007/s00360-015-0956-y

Hoff, M. L. M., Fabrizius, A., Czech-Damal, N. U., Folkow, L. P. and Burmester, T. (2017). Transcriptome analysis identifies key metabolic changes in the hooded seal (*Cystophora cristata*) brain in response to hypoxia and reoxygenation. *PLoS ONE* **12**, e0169366. doi:10.1371/journal.pone.0169366

Hylland, P., Milton, S., Pek, M., Nilsson, G. E. and Lutz, P. L. (1997). Brain Na+/K+-ATPase activity in two anoxia tolerant vertebrates: crucian carp and freshwater turtle. *Neurosci. Lett.* **235**, 89-92. doi:10.1016/S0304-3940(97)00727-1

Innis, S. M. (2005). Essential fatty acid metabolism during early development. *Biol. Grow. Anim.* **3**, 235-274. doi:10.1016/S1877-1823(09)70017-7

Irving, L. and Hart, J. S. (1957). The metabolism and insulation of seals as bare-skinned mammals in cold water. *Can. J. Zool.* **35**, 497-511. doi:10.1139/z57-041

Jin, J., Hou, Q., Mullen, T. D., Zeidan, Y. H., Bielawski, J., Kraveka, J. M., Bielawska, A., Obeid, L. M., Hannun, Y. A. and Hsu, Y.-T. (2008). Ceramide generated by sphingomyelin hydrolysis and the salvage pathway is involved in hypoxia/reoxygenation-induced Bax redistribution to mitochondria in NT-2 cells. *J. Biol. Chem.* **283**, 26509-26517. doi:10.1074/jbc.M801597200

Jurevics, H., Hostettler, J., Muse, E. D., Sammond, D. W., Matsushima, G. K., Toews, A. D. and Morell, P. (2001). Cerebroside synthesis as a measure of the rate of remyelination following cuprizone-induced demyelination in brain. *J. Neurochem.* **77**, 1067-1076. doi:10.1046/j.1471-4159.2001.00310.x

Kang, M. S., Ahn, K. H., Kim, S. K., Jeon, H. J., Ji, J. E., Choi, J. M., Jung, K. M., Jung, S. Y. and Kim, D. K. (2010). Hypoxia-induced neuronal apoptosis is mediated by de novo synthesis of ceramide through activation of serine palmitoyltransferase. *Cell. Signal.* **22**, 610-618. doi:10.1016/j.cellsig.2009.11.015

Kasamatsu, M., Kawauchi, R., Tsunokawa, M., Ueda, K., Uchida, E., Oikawa, S., Higuchi, H., Kawajiri, T., Uchida, S. and Nagahata, H. (2009). Comparison of serum lipid compositions, lipid peroxide, alpha-tocopherol and lipoproteins in captive marine mammals (bottlenose dolphins, spotted seals and West Indian manatees) and terrestrial mammals. *Res. Vet. Sci.* **86**, 216-222. doi:10.1016/j.rvsc.2008.07.006

Kasamatsu, M., Hasegawa, K., Wakabayashi, I., Seko, A. and Furuta, M. (2012). Hematology and serum biochemistry values in five captive finless porpoises (*Neophocaena phocaenoides*). *J. Vet. Med. Sci.* **74**, 1319-1322. doi:10.1292/jvms.11-0407

Kelly, P. A., Ford, I. and Mcculloch, J. (1986). The effect of diazepam upon local cerebral glucose use in the conscious rat. *Neuroscience* **19**, 257-265. doi:10.1016/0306-4522(86)90019-9

Kerem, D. and Elsner, R. (1973). Cerebral tolerance to asphyxial hypoxia in the harbor seal. Available online at *Respir. Physiol.* 19, 188-200. doi:10.1016/0034-5687(73)90077-7

Kohyama, K. and Inoshima, Y. (2017). Normal hematology and serum chemistry of northern fur seals (*Callorhinus ursinus*) in captivity. *Zoo. Biol.* **36**, 345-350. doi:10.1002/zoo.21376

Kolesnick, R. (1994). Signal transduction through the sphingomyelin pathway. *Mol. Chem. Neuropathol.* **21**, 287-297. doi:10.1007/BF02815356

Krüger, A., Fabrizius, A., Mikkelsen, B., Siebert, U., Folkow, L. P. and Burmester, T. (2020). Transcriptome analysis reveals a high aerobic capacity in the whale brain. *Comp. Biochem. Physiol. A Mol. Integr. Physiol.* **240**, 110593. doi:10.1016/j.cbpa.2019.110593

Kuhl, C., Tautenhahn, R., Böttcher, C., Larson, T. R. and Neumann, S. (2012). CAMERA: an integrated strategy for compound spectra extraction and annotation of liquid chromatography/mass spectrometry data sets. *Anal. Chem.* **84**, 283-289. doi:10.1021/ac202450g

Lauderdale, L. K., Walsh, M. T., Mitchell, K. A., Granger, D. A., Mellen, J. D. and Miller, L. J. (2021). Health reference intervals and values for common bottlenose dolphins (*Tursiops truncatus*), Indo-Pacific bottlenose dolphins (*Tursiops aduncus*), Pacific white-sided dolphins (*Lagenorhynchus obliquidens*), and beluga whales (*Delphinapterus leucas*). *PLoS ONE* **16**, e0250332. doi:10.1371/journal.pone.0250332

Law, B. A., Liao, X., Moore, K. S., Southard, A., Roddy, P., Ji, R., Szulc, Z., Bielawska, A., Schulze, P. C. and Cowart, L. A. (2018). Lipotoxic very-long-chain ceramides cause mitochondrial dysfunction, oxidative stress, and cell death in cardiomyocytes. *FASEB J.* **32**, 1403-1416. doi:10.1096/fj.201700300R

Lee, P., Chandel, N. S. and Simon, M. C. (2020). Cellular adaptation to hypoxia through hypoxia inducible factors and beyond. *Nat. Rev. Mol. Cell Biol.* **21**, 268-283. doi:10.1038/s41580-020-0227-y

Lehninger, A. L. (1981). *Biochemistry. The Molecular Basis of Cell Structure and Function*, 2nd edn. New York: Worth Publ.

Liao, W.-T., Liu, J., Zhou, S.-M., Xu, G., Gao, Y.-Q. and Liu, W.-Y. (2018). UHPLC-QTOFMS-based metabolomic analysis of the hippocampus in hypoxia preconditioned mouse. *Front. Physiol.* **9**, 1950. doi:10.3389/fphys.2018.01950

Libiseller, G., Dvorzak, M., Kleb, U., Gander, E., Eisenberg, T., Madeo, F., Neumann, S., Trausinger, G., Sinner, F., Pieber, T. et al. (2015). IPO: a tool for automated optimization of XCMS parameters. *BMC Bioinformatics* **16**, 118. doi:10.1186/s12859-015-0562-8

Liwanag, H. E. M., Berta, A., Costa, D. P., Budge, S. M. and Williams, T. M. (2012). Morphological and thermal properties of mammalian insulation: the evolutionary transition to blubber in pinnipeds. *Biol. J. Linn. Soc. Lond.* **107**, 774-787. doi:10.1111/j.1095-8312.2012.01992.x

Lutz, P. L. (2002). The Brain Without Oxygen. Causes of Failure-Physiological and Molecular Mechanisms for Survival. With assistance of G. E. Nilsson, H. M. Prentice. 3rd edn. Dordrecht: Springer Netherlands. Available online at https://ebookcentral.proquest.com/lib/kxp/detail.action?docID=6707121.

Manier, S. K., Keller, A. and Meyer, M. R. (2019). Automated optimization of XCMS parameters for improved peak picking of liquid chromatography-mass spectrometry data using the coefficient of variation and parameter sweeping for untargeted metabolomics. *Drug Test. Anal.* **11**, 752-761. doi:10.1002/dta.2552

Mazzaro, L. M., Lawrence Dunn, J., Furr, H. C. and Clark, R. M. (2003). Serum Retinol, alpha-tocopherol, and lipids in four species of adult captive pinnipeds. *Zoo Biol.* **22**, 83-96. doi:10.1002/zoo.10075

Meir, J. U., Champagne, C. D., Costa, D. P., Williams, C. L. and Ponganis, P. J. (2009). Extreme hypoxemic tolerance and blood oxygen depletion in diving elephant seals. *Am. J. Physiol. Regul. Integr. Comp. Physiol.* **297**, R927-R939. doi:10.1152/ajpregu.00247.2009

Meldrum, B. S. (2000). Glutamate as a neurotransmitter in the brain: review of physiology and pathology. *J. Nutr.* **130** Suppl. 4S, 1007S-1015S. doi:10.1093/jn/130.4.1007S

Mello, D. M. D., Melo, F. A. and Silva, V. M. F. (2021). Reference values for serum chemistry of wild Amazon river dolphins (*Inia geoffrensis*) from the central Amazon. *Mar. Mam. Sci.* **37**, 561-576. doi:10.1111/mms.12765

Mitz, S. A., Reuss, S., Folkow, L. P., Blix, A. S., Ramirez, J.-M., Hankeln, T. and Burmester, T. (2009). When the brain goes diving: glial oxidative metabolism may confer hypoxia tolerance to the seal brain. *Neuroscience* **163**, 552-560. doi:10.1016/j.neuroscience.2009.06.058

Monteiro, J. P., Maciel, E., Maia, R., Pereira, A. T., Calado, R., Domingues, P., Melo, T., Eira, C. and Domingues, M. R. (2021a). Characterization of the cardiac phospholipidome of small cetaceans provides adaptational insight and a foundation for indirect population health screening. *Mar. Mam. Sci.* **37**, 1406-1427. doi:10.1111/mms.12823

Monteiro, J. P., Maciel, E., Melo, T., Flanagan, C., Urbani, N., Neves, J. and Domingues, M. R. (2021b). The plasma phospholipidome of *Tursiops truncatus*: From physiological insight to the design of prospective tools for managed cetacean monitorization. *Lipids* **56**, 461-473. doi:10.1002/lipd.12307

Nabi, G., Robeck, T. R., Hao, Y. and Wang, D. (2019). Hematologic and biochemical reference interval development and the effect of age, sex, season, and location on hematologic analyte concentrations in critically endangered Yangtze finless porpoise (*Neophocaena asiaeorientalis* ssp. asiaeorientalis). *Front. Physiol.* **10**, 792. doi:10.3389/fphys.2019.00792

Noh, H. J., Turner-Maier, J., Schulberg, S. A., Fitzgerald, M. L., Johnson, J., Allen, K. N., Hückstädt, L. A., Batten, A. J., Alfoldi, J., Costa, D. P. et al. (2022). The Antarctic Weddell seal genome reveals evidence of selection on cardiovascular phenotype and lipid handling. *Commun. Biol.* **5**, 140. doi:10.1038/s42003-022-03089-2

Nollens, H. H., Haney, N. J., Stacy, N. I. and Robeck, T. R. (2020). Effects of sex, age, and season on the variation of blood analytes in a clinically healthy ex situ population of bottlenose dolphins (*Tursiops* spp.). *Vet. Q* **40**, 342-352. doi:10.1080/01652176.2020.1845415

Nollens, H. H., Robeck, T. R., Schmitt, T. L., Croft, L. L., Osborn, S. and Mcbain, J. F. (2019). Effect of age, sex, and season on the variation in blood analytes of a clinically normal ex situ population of killer whales (*Orcinus orca*). *Vet. Clin. Pathol.* **48**, 100-113. doi:10.1111/vcp.12697

Nordøy, E. S., Aakvaag, A. and Larsen, T. S. (1993). Metabolic adaptations to fasting in harp seal pups. *Physiol. Zool.* **66**, 926-945. doi:10.1086/physzool.66.6.30163747

Norman, S. A., Beckett, L. A., Miller, W. A., St Leger, J. and Hobbs, R. C. (2013). Variation in hematologic and serum biochemical values of belugas (*Delphinapterus leucas*) under managed care. *J. Zoo Wildl. Med.* **44**, 376-388. doi:10.1638/2012-0172R

Novgorodov, S. A., Voltin, J. R., Gooz, M. A., Li, L., Lemasters, J. J. and Gudz, T. I. (2018). Acid sphingomyelinase promotes mitochondrial dysfunction due to glutamate-induced regulated necrosis. *J. Lipid Res.* **59**, 312-329. doi:10.1194/jlr.M080374

Novgorodov, S. A., Voltin, J. R., Wang, W., Tomlinson, S., Riley, C. L. and Gudz, T. I. (2019). Acid sphingomyelinase deficiency protects mitochondria and improves function recovery after brain injury. *J. Lipid Res.* **60**, 609-623. doi:10.1194/jlr.M091132

O'Brien, J. S. and Sampson, E. L. (1965). Lipid composition of the normal human brain: gray matter, white matter, and myelin. *J. Lipid Res.* **6**, 537-544. doi:10.1016/S0022-2275(20)39619-X

Pang, Z., Chong, J., Zhou, G., Lima, M., De David, A., Le, C., Barrette, M., Jacques, P.-É., Li, S. and Xia, J. (2021). MetaboAnalyst 5.0: narrowing the gap between raw spectra and functional insights. *Nucleic Acids Res.* **49**, W388-W396. doi:10.1093/nar/gkab382

Parra, V., Eisner, V., Chiong, M., Criollo, A., Moraga, F., Garcia, A., Härtel, S., Jaimovich, E., Zorzano, A., Hidalgo, C. et al. (2008). Changes in mitochondrial dynamics during ceramide-induced cardiomyocyte early apoptosis. *Cardiovasc. Res.* **77**, 387-397. doi:10.1093/cvr/cvm029

Pellerin, L. and Magistretti, P. J. (1994). Glutamate uptake into astrocytes stimulates aerobic glycolysis: a mechanism coupling neuronal activity to glucose utilization. *Proc. Natl. Acad. Sci. U.S.A.* **91**, 10625-10629. doi:10.1073/pnas.91.22.10625

Pickles, S., Vigié, P. and Youle, R. J. (2018). Mitophagy and quality control mechanisms in mitochondrial maintenance. *Curr. Biol.* **28**, R170-R185. doi:10.1016/j.cub.2018.01.004

Piomelli, D., Astarita, G. and Rapaka, R. (2007). A neuroscientist's guide to lipidomics. *Nat. Rev. Neurosci.* **8**, 743-754. doi:10.1038/nrn2233

Ponganis, P. J. (2011). Diving mammals. *Comp. Physiol.* **1**, 447-465. doi:10.1002/cphy.c091003

Prando, S., Carneiro, C. d. G., Otsuki, D. A. and Sapienza, M. T. (2019). Effects of ketamine/xylazine and isoflurane on rat brain glucose metabolism measured by 18 F-fluorodeoxyglucose-positron emission tomography. *Eur. J. Neurosci.* **49**, 51-61. doi:10.1111/ejn.14252

Qvist, J., Hill, R. D., Schneider, R. C., Falke, K. J., Liggins, G. C., Guppy, M., Elliot, R. L., Hochachka, P. W. and Zapol, W. M. (1986). Hemoglobin concentrations and blood gas tensions of free-diving Weddell seals. *J. Appl. Physiol.* **61**, 1560-1569. doi:10.1152/jappl.1986.61.4.1560

Ramirez, J.-M., Folkow, L. P. and Blix, A. S. (2007). Hypoxia tolerance in mammals and birds: from the wilderness to the clinic. *Annu. Rev. Physiol.* **69**, 113-143. doi:10.1146/annurev.physiol.69.031905.163111

Ramirez, J.-M., Folkow, L. P., Ludvigsen, S., Ramirez, P. N. and Blix, A. S. (2011). Slow intrinsic oscillations in thick neocortical slices of hypoxia tolerant deep diving seals. *Neuroscience* **177**, 35-42. doi:10.1016/j.neuroscience.2010.12.032.

Rey, F., Melo, T., Lopes, D., Couto, D., Marques, F. and Domingues, M. R. (2022). Applications of lipidomics in marine organisms: progress, challenges and future perspectives. *Mol. Omics* **18**, 357-386. doi:10.1039/D2MO00012A

Ruiz-Hernández, I. M., Nouri, M.-Z., Kozuch, M., Denslow, N. D., Díaz-Gamboa, R. E., Rodríguez-Canul, R. and Collí-Dulá, R. C. (2022). Trace element and lipidomic analysis of bottlenose dolphin blubber from the Yucatan coast: Lipid composition relationships. *Chemosphere* **299**, 134353. doi:10.1016/j.chemosphere.2022.134353

Schlegel, R. A. and Williamson, P. (2001). Phosphatidylserine, a death knell. *Cell Death Differ.* **8**, 551-563. doi:10.1038/sj.cdd.4400817

Schneider, N., Hauser, J., Oliveira, M., Cazaubon, E., Mottaz, S. C., O'neill, B. V., Steiner, P. and Deoni, S. C. L. (2019). Sphingomyelin in brain and cognitive development: preliminary data. *eNeuro* **6**, 4. doi:10.1523/ENEURO.0421-18.2019

Scholander, P. F. (1940). *Experimental investigations on the respiratory function in diving mammals and birds*. Oslo: Dybwad.

Schousboe, A. (1981). Transport and metabolism of glutamate and GABA in neurons and glial cells. *Int. Rev. Neurobiol.* **22**, 1-45. doi:10.1016/S0074-7742(08)60289-5

Sentelle, R. D., Senkal, C. E., Jiang, W., Ponnusamy, S., Gencer, S., Selvam, S. P., Ramshesh, V. K., Peterson, Y. K., Lemasters, J. J., Szulc, Z. M. et al. (2012). Ceramide targets autophagosomes to mitochondria and induces lethal mitophagy. *Nat. Chem. Biol.* **8**, 831-838. doi:10.1038/nchembio.1059

Shimizu, S., Narita, M. and Tsujimoto, Y. (1999). Bcl-2 family proteins regulate the release of apoptogenic cytochrome c by the mitochondrial channel VDAC. *Nature* **399**, 483-487. doi:10.1038/20959

Simond, A. E., Houde, M., Lesage, V., Michaud, R. and Verreault, J. (2020). Metabolomic profiles of the endangered St. Lawrence Estuary beluga population and associations with organohalogen contaminants. *Sci. Total Environ.* **717**, 137204. doi:10.1016/j.scitotenv.2020.137204

Simond, A. É., Noël, M., Loseto, L., Houde, M., Kirk, J., Elliott, A. and Brown, T. M. (2022). A Multi-matrix metabolomic approach in ringed seals and beluga whales to evaluate contaminant and climate-related stressors. *Metabolites* **12**, 813. doi:10.3390/metabo12090813

Siskind, L. J., Kolesnick, R. N. and Colombini, M. (2002). Ceramide channels increase the permeability of the mitochondrial outer membrane to small proteins. *J. Biol. Chem.* **277**, 26796-26803. doi:10.1074/jbc.M200754200

Smith, C. A., Want, E. J., O'maille, G., Abagyan, R. and Siuzdak, G. (2006). XCMS: processing mass spectrometry data for metabolite profiling using nonlinear peak alignment, matching, and identification. *Anal. Chem.* **78**, 779-787. doi:10.1021/ac051437y

Steinman, K. J., Robeck, T. R., Fetter, G. A., Schmitt, T. L., Osborn, S., Dirocco, S., Nollens, H. H. and O'Brien, J. K. (2020). Circulating and excreted corticosteroids and metabolites, hematological, and serum chemistry parameters in the killer whale (*Orcinus orca*) before and after a stress response. *Front. Mar. Sci.* **6**, 830. doi:10.3389/fmars.2019.00830

Strandberg, U., Käkelä, A., Lydersen, C., Kovacs, K. M., Grahl-Nielsen, O., Hyvärinen, H. and Käkelä, R. (2008). Stratification, composition, and function of marine mammal blubber: the ecology of fatty acids in marine mammals. *Physiol. Biochem. Zool.* **81**, 473-485. doi:10.1086/589108

Sud, M., Fahy, E., Cotter, D., Azam, K., Vadivelu, I., Burant, C., Edison, A., Fiehn, O., Higashi, R., Nair, K. S. et al. (2016). Metabolomics Workbench: An international repository for metabolomics data and metadata, metabolite standards, protocols, tutorials and training, and analysis tools. *Nucleic Acids Res.* **44**, D463-D470. doi:10.1093/nar/gkv1042

Swanson, R. A. and Choi, D. W. (1993). Glial glycogen stores affect neuronal survival during glucose deprivation in vitro. *J. Cereb. Blood Flow Metab.* **13**, 162-169. doi:10.1038/jcbfm.1993.19

Tang, C.-H., Lin, C.-Y., Tsai, Y.-L., Lee, S.-H. and Wang, W.-H. (2018). Lipidomics as a diagnostic tool of the metabolic and physiological state of managed whales: A correlation study of systemic metabolism. *Zoo Biol.* **37**, 440-451. doi:10.1002/zoo.21452

Tift, M. S., Houser, D. S. and Crocker, D. E. (2011). High-density lipoprotein remains elevated despite reductions in total cholesterol in fasting adult male elephant seals (*Mirounga angustirostris*). *Comp. Biochem. Physiol. B Biochem. Mol. Biol.* **159**, 214-219. doi:10.1016/j.cbpb.2011.04.005

Trumble, S. J., Noren, S. R., Cornick, L. A., Hawke, T. J. and Kanatous, S. B. (2010). Age-related differences in skeletal muscle lipid profiles of Weddell seals: clues to developmental changes. *J. Exp. Biol.* **213**, 1676-1684. doi:10.1242/jeb.040923

Tsai, Y.-L., Chen, S.-Y., Lin, S.-C. and Li, J.-Y. (2016). Effects of physiological factors and seasonal variations on hematology and plasma biochemistry of beluga whales (*Delphinapterus leucas*) managed in pingtung. *Taiwan. Aquatic Mamm* **42**, 494-506. doi:10.1578/AM.42.4.2016.494

Tsujimoto, Y. and Shimizu, S. (2000). VDAC regulation by the Bcl-2 family of proteins. *Cell Death Differ.* **7**, 1174-1181. doi:10.1038/sj.cdd.4400780

Vacquie-Garcia, J., Lydersen, C., Biuw, M., Haug, T., Fedak, M. A. and Kovacs, K. M. (2017). Hooded seal *Cystophora cristata* foraging areas in the Northeast Atlantic Ocean-Investigated using three complementary methods. *PLoS ONE* **12**, e0187889. doi:10.1371/journal.pone.0187889

Van Blitterswijk, W. J., Van Der Luit, A. H., Veldman, R. J., Verheij, M. and Borst, J. (2003). Ceramide: second messenger or modulator of membrane structure and dynamics? *Biochem. J.* **369**, 199-211. doi:10.1042/BJ20021528

Van Meer, G., Voelker, D. R. and Feigenson, G. W. (2008). Membrane lipids: where they are and how they behave. *Nat. Rev. Mol. Cell Biol.* **9**, 112-124. doi:10.1038/nrm2330

Venn-Watson, S., Smith, C. R. and Jensen, E. D. (2008). Assessment of increased serum aminotransferases in a managed Atlantic bottlenose dolphin (*Tursiops truncatus*) population. *J. Wildl. Dis.* **44**, 318-330. doi:10.7589/0090-3558-44.2.318

Watson, D. G., Pomeroy, P. P. and Kennedy, M. W. (2021). Atlantic grey seal milk shows continuous changes in key metabolites and indicators of metabolic transition in pups from birth to weaning. *Front. Mar. Sci.* **7**, 596904. doi:10.3389/fmars.2020.596904

Wheatley, K. E., Bradshaw, C. J. A., Harcourt, R. G., Davis, L. S. and Hindell, M. A. (2006). Chemical immobilization of adult female Weddell seals with tiletamine and zolazepam: effects of age, condition and stage of lactation. *BMC Vet. Res.* **2**, 8. doi:10.1186/1746-6148-2-8

Wheatley, K. E., Nichols, P. D., Hindell, M. A., Harcourt, R. G. and Bradshaw, C. J. A. (2008). Differential mobilization of blubber fatty acids in lactating Weddell seals: evidence for selective use. *Physiol. Biochem. Zool* **81**, 651-662. doi:10.1086/590397

Williams, E. E., Stewart, B. S., Beuchat, C. A., Somero, G. N. and Hazel, J. R. (2001). Hydrostatic-pressure and temperature effects on the molecular order of erythrocyte membranes from deep-, shallow-, and non-diving mammals. *Can. J. Zool.* **79**, 888-894. doi:10.1139/cjz-79-5-888

Witting, M., Ruttkies, C., Neumann, S. and Schmitt-Kopplin, P. (2017). LipidFrag: improving reliability of in silico fragmentation of lipids and application to the *Caenorhabditis elegans* lipidome. *PLoS ONE* **12**, e0172311. doi:10.1371/journal.pone.0172311

Wolf, S., Schmidt, S., Müller-Hannemann, M. and Neumann, S. (2010). In silico fragmentation for computer assisted identification of metabolite mass spectra. *BMC Bioinformatics* **11**, 148. doi:10.1186/1471-2105-11-148

Xia, J., Psychogios, N., Young, N. and Wishart, D. S. (2009). MetaboAnalyst: a web server for metabolomic data analysis and interpretation. *Nucleic Acids Res.* **37**, W652-W660. doi:10.1093/nar/gkp356

Yu, Z. F., Nikolova-Karakashian, M., Zhou, D., Cheng, G., Schuchman, E. H. and Mattson, M. P. (2000). Pivotal role for acidic sphingomyelinase in cerebral ischemia-induced ceramide and cytokine production, and neuronal apoptosis. *J. Mol. Neurosci.* **15**, 85-98. doi:10.1385/JMN:15:2:85

Zhao, Y., Calon, F., Julien, C., Winkler, J. W., Petasis, N. A., Lukiw, W. J. and Bazan, N. G. (2011). Docosahexaenoic acid-derived neuroprotectin D1 induces neuronal survival via secretase- and PPARγ-mediated mechanisms in Alzheimer's disease models. *PLoS ONE* **6**, e15816. doi:10.1371/journal.pone.0015816

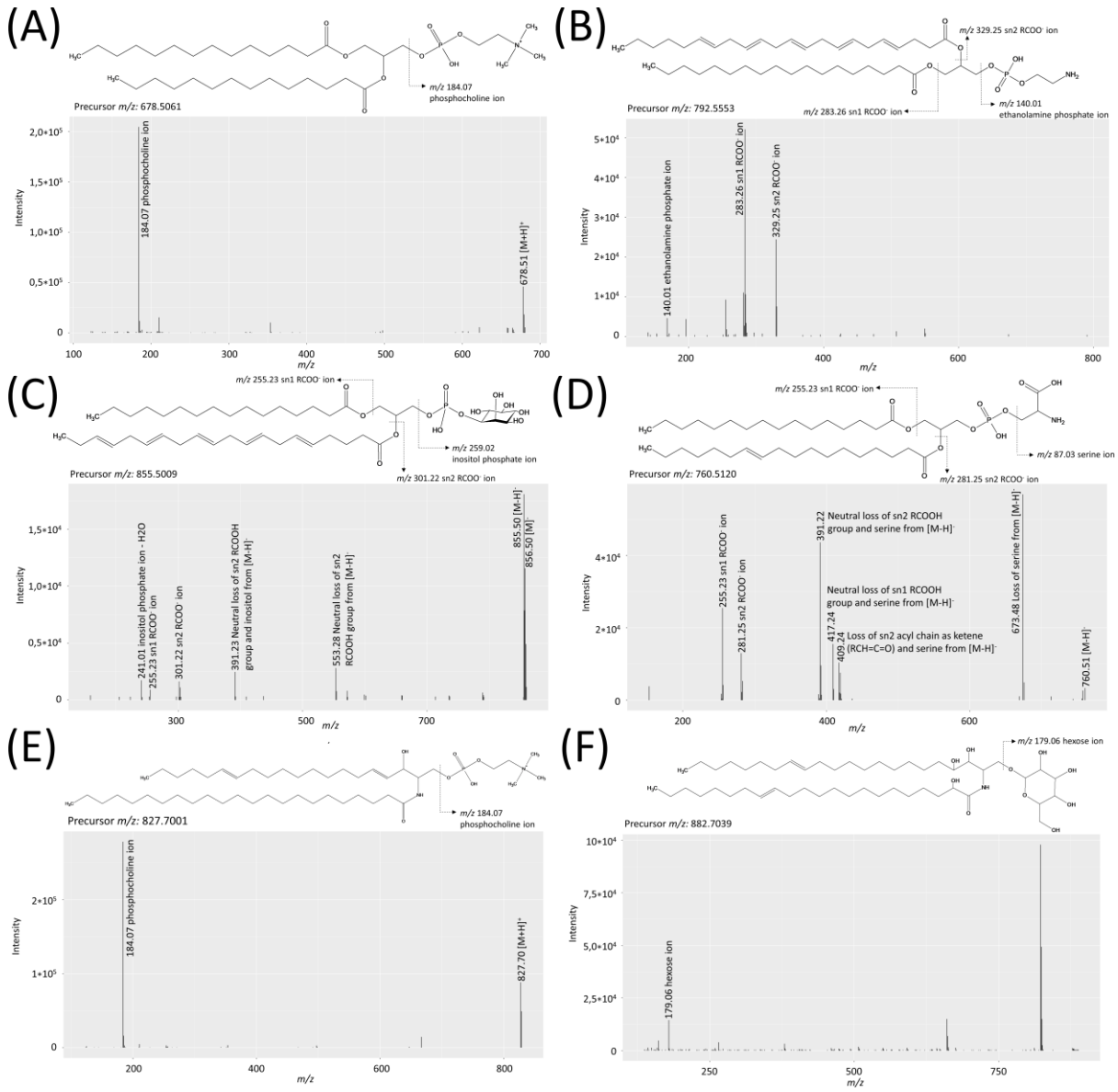

Fig. S1. MS/MS spectra of **(A)** PC(28:0) measured in positive ionization mode, **(B)** PE(40:5) measured in negative ionization mode, **(C)** PI(36:5) measured in negative ionization mode, **(D)** PS(34:1) measured in negative ionization mode, **(E)** SM(d43:2) measured in positive ionization mode and **(F)** HexCer(d44:2) measured in negative ionization mode**.**

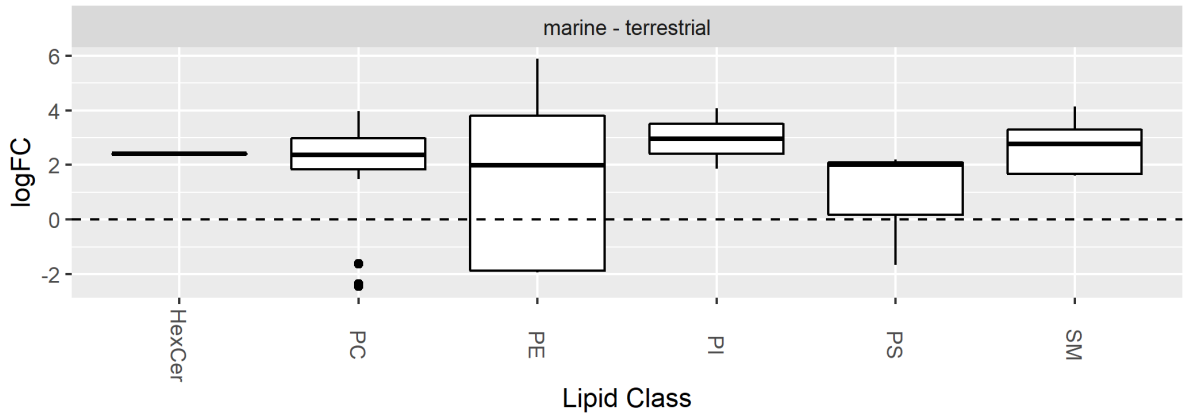

Fig. S2. Fold change of lipid classes between marine and terrestrial mammals. The dashed line indicates the value (logFC = 0), at which lipids are present in equal concentrations in marine and terrestrial mammals. Positive logFC values represent higher abundance in marine mammals, while negative logFC values describe increase in terrestrial mammals. PC: phosphatidylcholine; PE: phosphatidylethanolamine; PI: phospatidylinositol; PS: phosphatidylserine; SM: sphingomylein; HexCer: cerebroside. Please refer to Table S1 for amount of detected lipid species in each lipid class. No significant differences were determined.

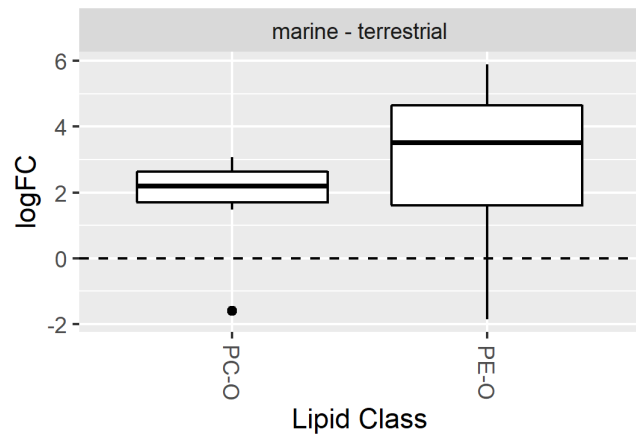

Fig. S3. Fold change of plasmalogen lipid classes between marine and terrestrial mammals. The dashed line indicates the value (logFC = 0), at which lipids are present in equal concentrations in marine and terrestrial mammals. Positive logFC values represent higher abundance in marine mammals, while negative logFC values describe increase in terrestrial mammals. PC-O: phosphatidylcholine plasmalogen; PE-O: phosphatidylethanolamine plasmalogen. Please refer to Table S1 for amount of detected lipid species in each lipid class. No significant differences were determined.

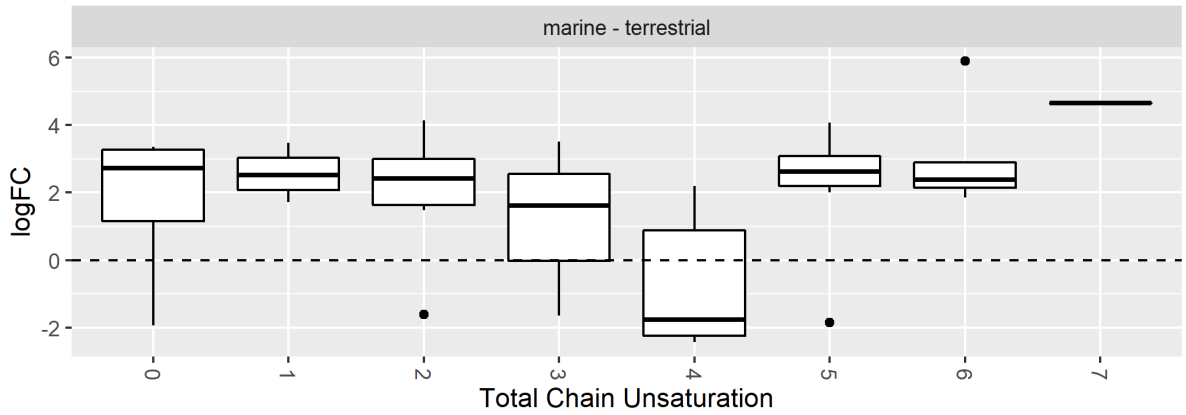

Fig S4. Fold change of fatty acid unsaturation of identified lipids between marine and terrestrial mammals. The dashed line indicates the value (logFC = 0), at which lipids are present in equal concentrations in marine and terrestrial mammals. Positive logFC values represent higher abundance in marine mammals, while negative logFC values describe increase in terrestrial mammals. Please refer to Table S1 for amount of detected lipid species within each total chain unsaturation. No significant differences were determined.

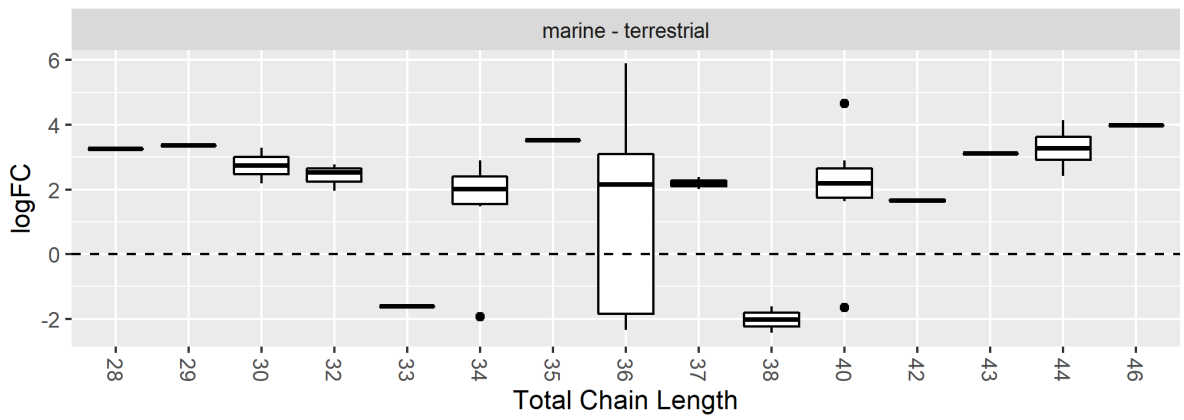

Fig. S5. Fold change of fatty acid chain length of identified lipids between marine and terrestrial mammals. The dashed line indicates the value (logFC = 0), at which lipids are present in equal concentrations in marine and terrestrial mammals. Positive logFC values represent higher abundance in marine mammals, while negative logFC values describe increase in terrestrial mammals. Please refer to Table S1 for amount of detected lipid species within each total chain length. No significant differences were determined.

Table S1. Detected lipids with annotation from MS/MS spectra including adduct, mass, MetFrag and LipidFrag scores. Fold change (log2FC) and false discovery rate (FDR) were calculated from MS spectra. Positive log2FC values represent higher abundance in marine mammals (↑), while negative log2FC values describe lower abundance in comparison to the terrestrial mammals (↓). Error between measured, i.e., detected *m/z* in mass spectrometry, and calculated, i.e., expected *m/z* from molecular formula, is given in parts per million (ppm). The optimum MetFrag as well as LipidFrag score of 1.0 represents a likely lipid identification, while lower scores indicate weaker annotation confidence. PC: phosphatidylcholine; PE: phosphatidylethanolamine; PI: phospatidylinositol; PS: phosphatidylserine; SM: sphingomylein; HexCer: cerebroside.

Tentative compound	Proposed formula	Retention time [min]	Adduct	*m/z* measured	*m/z* calculated	Error [ppm]	Relevant fragments	MetFrag Score	LipidFrag Score	log2FC	FDR
Glycerophospholipids											
PC(28:0)	$C_{36}H_{72}NO_8P$	9.3	$[M+H]^+$	678.5065	678.5068	-0.4	184.07: $C_5H_{13}NO_4P$	1.0	0.6	2.9↑	<0.0001
PC(29:0)	$C_{37}H_{74}NO_8P$	9.8	$[M+H]^+$	692.5223	692.5225	-0.3	184.07: $C_5H_{13}NO_4P$	1.0	0.5	3.3↑	<0.0001
PC(30:1)	$C_{38}H_{74}NO_8P$	9.5	$[M+H]^+$	704.5222	704.5225	-0.4	184.07: $C_5H_{13}NO_4P$	1.0	0.6	2.9↑	<0.0001
PC(32:2)	$C_{40}H_{76}NO_8P$	9.7	$[M+H]^+$	730.5378	730.5381	-0.4	184.07: $C_5H_{13}NO_4P$	1.0	0.5	2.0↑	<0.0001
PC(33:4)	$C_{41}H_{74}NO_8P$	11.1	$[M+H]^+$	740.5218	740.5225	-0.9	184.07: $C_5H_{13}NO_4P$	0.5	1.0	-1.5↓	<0.0001
PC(36:4)	$C_{44}H_{80}NO_8P$	10.8	$[M+H]^+$	782.5708	782.5694	1.7	184.07: $C_5H_{13}NO_4P$	1.0	0.5	-1.6↓	0.0122
PC(36:5)	$C_{44}H_{78}NO_8P$	9.9	$[M+H]^+$	780.5535	780.5538	-0.4	184.07: $C_5H_{13}NO_4P$	1.0	0.6	2.8↑	<0.0001
PC(36:5)	$C_{44}H_{78}NO_8P$	10.1	$[M+H]^+$	780.5536	780.5538	-0.3	184.07: $C_5H_{13}NO_4P$	1.0	0.5	3.4↑	<0.0001
PC(36:6)	$C_{44}H_{76}NO_8P$	9.5	$[M+H]^+$	778.5380	778.5381	-0.1	184.07: $C_5H_{13}NO_4P$; 433.3:	1.0	0.6	2.4↑	<0.0001
PC(37:5)	$C_{45}H_{80}NO_8P$	12.3	$[M+H]^+$	794.5690	794.5694	-0.5	184.07: $C_5H_{13}NO_4P$	1.0	0.6	2.2↑	0.0025
PC(37:6)	$C_{45}H_{78}NO_8P$	10.0	$[M+H]^+$	792.5536	792.5538	-0.2	184.07: $C_5H_{13}NO_4P$	1.0	0.6	2.5↑	<0.0001
PC(38:4)	$C_{46}H_{84}NO_8P$	11.5	$[M+H]^+$	810.6002	810.6007	-0.6	184.07: $C_5H_{13}NO_4P$	1.0	0.7	-1.7↓	0.0068
PC(40:6)	$C_{48}H_{84}NO_8P$	11.2	$[M+H-H_2O]^+$	816.5884	816.5878	0.7	184.07: $C_5H_{13}NO_4P$	-	-	2.9↑	<0.0001
PC(46:2)	$C_{54}H_{104}NO_8P$	16.4	$[M+H]^+$	926.7522	926.7572	-5.4	184.07: $C_5H_{13}NO_4P$	1.0	0.5	3.7↑	0.0001
PC(O-30:0)	$C_{38}H_{78}NO_7P$	11.1	$[M+H]^+$	692.5581	692.5589	-1.2	184.07: $C_5H_{13}NO_4P$	1.0	0.0	2.2↑	<0.0001
PC(O-32:1)	$C_{40}H_{80}NO_7P$	11.3	$[M+H]^+$	718.5742	718.5745	-0.5	184.07: $C_5H_{13}NO_4P$	0.6	0.0	2.5↑	<0.0001
PC(O-34:1)	$C_{42}H_{84}NO_7P$	12.0	$[M+H-H_2O]^+$	728.6027	728.5952	10.3	184.07: $C_5H_{13}NO_4P$	-	-	2.9↑	0.0012
PC(O-34:2)	$C_{42}H_{82}NO_7P$	10.6	$[M+Cl]^-$	778.5582	778.5523	7.6	168.04: $C_4H_{10}NO_4P$; 255.23: $C_{16}H_{28}O_2$	0.7	0.0	1.5↑	0.0015
PC(O-34:2)	$C_{42}H_{82}NO_7P$	11.4	$[M+H]^+$	744.5895	744.5902	-1.0	184.07: $C_5H_{13}NO_4P$	1.0	0.0	2.7↑	<0.0001
PC(O-34:2)	$C_{42}H_{82}NO_7P$	12.2	$[M+H]^+$	744.5877	744.5902	-3.3	184.07: $C_5H_{13}NO_4P$	-	-	3.6↑	<0.0001
PC(O-36:4)	$C_{44}H_{82}NO_7P$	12.0	$[M+H-H_2O]^+$	750.5862	750.5796	8.7	184.07: $C_5H_{13}NO_4P$	-	-	2.0↑	0.0002
PC(O-38:2)	$C_{46}H_{90}NO_7P$	13.9	$[M+H-H_2O]^+$	782.6485	782.6422	8.0	184.07: $C_5H_{13}NO_4P$	-	-	-1.0↓	0.0357
PC(O-44:5)	$C_{52}H_{96}NO_7P$	15.1	$[M+H-H_2O]^+$	860.6940	860.6891	5.7	184.07: $C_5H_{13}NO_4P$	-	-	3.2↑	<0.0001
PE(34:0)	$C_{39}H_{78}NO_8P$	12.4	$[M-H]^-$	718.5372	718.5392	-2.7	255.23: $C_{16}H_{30}O_2$; 283.26: $C_{18}H_{34}O_2$	1.0	1.0	-1.5↓	0.0001
PE(36:4)	$C_{41}H_{74}NO_8P$	10.7	$[M-H]^-$	738.5073	738.5079	-0.8	255.23: $C_{16}H_{31}O_2$; 303.23: $C_{20}H_{31}O_2$	1.0	1.0	-1.7↓	<0.0001
PE(40:5)	$C_{45}H_{80}NO_8P$	11.8	$[M-H]^-$	792.5534	792.5549	-1.9	140.01: $C_2H_7NO_4P$; 283.26: $C_{18}H_{33}O_2$; 329.25: $C_{22}H_{34}O_2$	1.0	1.0	2.5↑	<0.0001

PE(O-34:3)	$C_{39}H_{74}NO_7P$	11.6	$[M-H]^-$	698.5107	698.5130	-3.3	253.22: $C_{16}H_{26}O_2$; 283.26: $C_{18}H_{34}O_2$	1.0	0.0	2.0↑	0.0024
PE(O-35:3)	$C_{40}H_{76}NO_7P$	11.8	$[M-H]^-$	712.5266	712.5285	-2.6	267.23: $C_{17}H_{29}O_2$; 281.25: $C_{18}H_{30}O_2$	1.0	0.0	4.0↑	<0.0001
PE(O-36:5)	$C_{41}H_{74}NO_7P$	11.2	$[M-H]^-$	722.5115	722.5130	-2.1	303.23: $C_{20}H_{31}O_2$; 436.28: $C_{21}H_{43}NO_6P$	1.0	0.0	-1.7↓	<0.0001
PE(O-36:6)	$C_{41}H_{72}NO_7P$	10.6	$[M-H]^-$	720.4954	720.4974	-2.8	301.22: $C_{20}H_{29}O_2$; 436.28: $C_{21}H_{43}NO_6P$	1.0	0.0	5.5↑	<0.0001
PE(O-40:7)	$C_{45}H_{78}NO_7P$	11.4	$[M-H]^-$	774.5427	774.5443	-2.0	140.01: $C_2H_7NO_4P$; 283.24: $C_{21}H_{31}$; 327.23: $C_{22}H_{31}O_2$	1.0	0.0	4.2↑	<0.0001
PI(36:5)	$C_{45}H_{77}O_{13}P$	6.7	$[M-H]^-$	855.5014	855.5029	-1.8	241.01: $C_6H_{11}O_8P$; 301.22: $C_{20}H_{29}O_2$; 391.23: $C_{19}H_{37}O_6P$; 553.28: $C_{25}H_{47}O_{11}P$	1.0	1.0	4.0↑	<0.0001
PI(40:6)	$C_{49}H_{83}O_{13}P$	7.2	$[M-H]^-$	909.5493	909.5499	-0.7	283.26: $C_{18}H_{35}O_2$; 419.26: $C_{21}H_{41}O_6P$; 581.31: $C_{27}H_{51}O_{11}P$	1.0	1.0	2.0↑	0.0003
PS(34:1)	$C_{40}H_{76}NO_{10}P$	7.9	$[M-H]^-$	760.5118	760.5134	-2.1	255.23: $C_{16}H_{31}O_2$; 281.25: $C_{18}H_{33}O_2$; 391.22: $C_{19}H_{37}O_6P$; 409.24: $C_{19}H_{37}O_7P$; 417.24: $C_{21}H_{39}O_6P$; 673.48: $C_{37}H_{70}O_8P$	1.0	1.0	2.1↑	<0.0001
PS(40:3)	$C_{46}H_{84}NO_{10}P$	10.4	$[M-H]^-$	840.5756	840.5760	-0.5	283.26: $C_{18}H_{33}O_2$; 419.26: $C_{21}H_{39}O_6P$; 437.27: $C_{21}H_{39}O_7P$; 753.54: $C_{43}H_{78}O_8P$	1.0	1.0	-1.3↓	0.0002
PS(40:4)	$C_{46}H_{82}NO_{10}P$	9.8	$[M-H]^-$	838.5583	838.5604	-2.5	283.26: $C_{18}H_{35}O_2$; 331.26: $C_{22}H_{35}O_2$; 419.26: $C_{21}H_{41}O_6P$; 437.27: $C_{21}H_{41}O_7P$; 467.26: $C_{25}H_{41}O_6P$; 751.53: $C_{43}H_{76}O_8P$	1.0	1.0	2.1↑	0.0001
						Sphingolipids					
SM(d32:1)	$C_{37}H_{75}N_2O_6P$	9.3	$[M+H]^+$	675.5433	675.5435	-0.3	184.07: $C_5H_{13}NO_4P$	1.0	0.0	2.4↑	<0.0001
SM(d40:2)	$C_{45}H_{89}N_2O_6P$	12.6	$[M+H]^+$	785.6521	785.6535	-1.8	184.07: $C_5H_{13}NO_4P$	1.0	0.0	2.2↑	0.0056
SM(d42:1)	$C_{47}H_{95}N_2O_6P$	14.7	$[M+H]^+$	815.6995	815.7000	-0.6	184.07: $C_5H_{13}NO_4P$	1.0	0.0	2.3↑	0.0182
SM(d42:2)	$C_{47}H_{93}N_2O_6P$	13.7	$[M+Na]^+$	835.6653	835.6663	-1.2	184.07: $C_5H_{13}NO_4P$	1.0	0.0	2.3↑	0.0137
SM(d43:2)	$C_{48}H_{95}N_2O_6P$	14.2	$[M+H]^+$	827.6985	827.7000	-1.9	184.07: $C_5H_{13}NO_4P$	1.0	0.0	3.2↑	0.0065
SM(d44:1)	$C_{49}H_{99}N_2O_6P$	15.6	$[M+H]^+$	843.7301	843.7313	-1.5	184.07: $C_5H_{13}NO_4P$	-	-	2.6↑	0.0005
SM(d44:2)	$C_{49}H_{97}N_2O_6P$	14.6	$[M+H]^+$	841.7147	841.7157	-1.2	184.07: $C_5H_{13}NO_4P$	1.0	0.0	3.3↑	0.0001
HexCer(d44:2	$C_{50}H_{95}NO_8$	14.0	$[M+Formate]^-$	882.7026	882.7040	-1.6	179.06: $C_6H_{12}O_6$	-	-	3.2↑	0.0146